International Journal of Nanomedicine

Dovepress
Taylor & Francis Group

Open Access Full Text Article

REVIEW

Removing Barriers to Tumor 'Oxygenation': Depleting Glutathione Nanozymes in Cancer Therapy

Ruilong Sun[1–3], Ruitang Liu[1,2], Yongzheng Tian[1], Yunfei Li[1], Bo Fan[1], Songkai Li[1]

[1]Spine Surgery, The 940th Hospital of the Joint Logistic Support Force of Chinese People's Liberation Army, Lanzhou, People's Republic of China; [2]First Clinical Medical College, Gansu University of Chinese Medicine, Lanzhou, People's Republic of China; [3]Gansu Provincial Key Laboratory of Stem Cells and Gene Drugs, Lanzhou, People's Republic of China

Correspondence: Bo Fan; Songkai Li, Email qlsjhjpdnl@163.com; wangyizhe1226@163.com

Abstract: Nanozymes are nanomaterials capable of mimicking natural enzyme catalysis in the complex biological environment of the human body. Due to their good stability and strong catalytic properties, nanozymes are widely used in various fields of biomedicine. Among them, nanozymes that trigger intracellular reactive oxygen species (ROS) levels for cancer therapy have gained significant attention. However, the 'explosion' of ROS in tumor cells was prevented by the high levels of glutathione (GSH) in the tumor microenvironment (TME). GSH, a prominent endogenous antioxidant, increases the resistance of tumor cells to oxidative stress by scavenging ROS. Certain nanozymes can deplete intracellular GSH levels by mimicking GSH oxidase (GSHOx), GSH peroxidase (GPx) or by interfering with the reduction of oxidized glutathione (GSSG). On the one hand, elevated the level of intracellular ROS and induced lipid peroxidation reaction leading to ferroptosis. On the other hand, it creates favorable conditions for the treatment of tumors with photodynamic therapy (PDT), sonodynamic therapy (SDT), chemodynamical therapy (CDT) and targeted therapy. In this paper, we present a comprehensive analysis of GSH-depleting nanozymes reported in recent years, including classification, mechanism, responsiveness to TME and their roles in cancer therapy, and look forward to future applications and developments.

Keywords: nanomaterials, enzyme mimetic, nanozymes, glutathione depletion, oxygen-dependent therapy, cancer therapy

Introduction

Cancer is a leading cause of death worldwide, with almost 10 million deaths reported in 2020.[1] By 2030, it is projected that there will be 13.1 million deaths related to cancer (World Health Organization, WHO, http://www.who.int/en/). Major challenges in cancer treatment include tumor recurrence, metastasis and resistance to chemotherapeutic agents.[2–5] Chemotherapy, radiotherapy and surgery are currently the most effective treatments, but these traditional approaches have major limitations, including potential damage to healthy cells, tumor recurrence, poor visibility and tumor hypoxia.[6–8] The development of new chemotherapeutic agents to combat cancer has received great attention as a research hotspot.

Like other areas of research, nanotechnology is an area of intense interest in cancer diagnosis and treatment. In recent years, the use of nanomaterials in ODCT has gained a considerable amount of attention, eg PDT, SDT and CDT are used to treat a variety of diseases such as cancer, infection and inflammation.[9–11] Compared to conventional therapies, ODCT showed high selectivity, modifiability, and low levels of systemic toxicity.[12,13] However, tumor hypoxia, which is the insufficient levels of oxygen within the TME, has been found to reduce the efficacy of ODCT.[14] Nanozymes are a type of nanomaterial that exhibit enzyme-like activity. Various nanozymes, such as mimetic catalase (CAT), oxidase (OXD), peroxidase (POD), and superoxide dismutase (SOD), have been explored as potential therapies for cancer treatment.[15] They can achieve direct killing by increasing the level of ROS and indirect killing by depleting ROS.[16]

Lack of GSH, a key antioxidant in the antioxidant system, disturbs the redox balance of tumor cells, leading to ROS accumulation, cell damage and even death.[17–19] Various nanozymes have been reported to deplete intracellular GSH levels or inhibit GSH production, resulting in reduced GSH clearance of ROS, thereby maintaining the state of oxidative

Received: 4 January 2025
Accepted: 12 April 2025
Published: 1 May 2025

stress in tumor cells and enhancing the efficacy of ODCT.[20,21] The depletion of GSH induced by the nanozymes has been associated with both ferroptosis and apoptosis as well as increased sensitivity to chemo- and radiotherapeutic drugs.[22–24] Ferroptosis due to ROS accumulation and GSH-dependent GPX4 inactivation has emerged as a regulated form of cell death in cancer therapy.[25,26] However, there is a lack of detailed review on nanozymes depleting GSH in cancer therapy. This paper reviews the current status and prospects of nanozymes depleting GSH in cancer therapy (Figure 1).

Enzymes and Nanozymes

Natural enzymes act as biocatalysts for various biological reactions in vivo, controlling nutrient metabolism, energy conversion, and disease processes. However, the practical application of natural enzymes is greatly restricted due to their inherent limitations, such as poor stability, high production costs, and difficulty in recycling[27–29] (Table 1). To address this issue, researchers have introduced artificial enzymes that imitate the activity of natural enzymes. POD-mimicking Fe_3O_4 nanoparticles (NPs) were first discovered by Yan et al in 2007.[30] And since then, nanozymes have gained widespread attention for their modulatability, high reactivity, multifunctionality and intrinsic biocatalytic ROS generation and scavenging activities.[31–33] In addition, nanozymes' catalytic activity can be adjusted by altering their structure, shape, and composition and nanomaterials have been successfully used to mimic the catalytic activities of several natural enzymes (eg CAT, OXD, POD, SOD, etc).[34–38] Nanozymes have a wide range of applications in fields such as energy, environment, antimicrobial agents, biosensing, and disease treatment due to their unique properties. Their efficient catalytic activity enables the effective elimination of organic pollutants and heavy metals, thereby enhancing the efficiency and sustainability of environmental treatment.[39–41] Moreover, nanozymes are a promising solution to the problem of bacterial drug resistance: they act as antimicrobial agents by catalysing the production of highly active

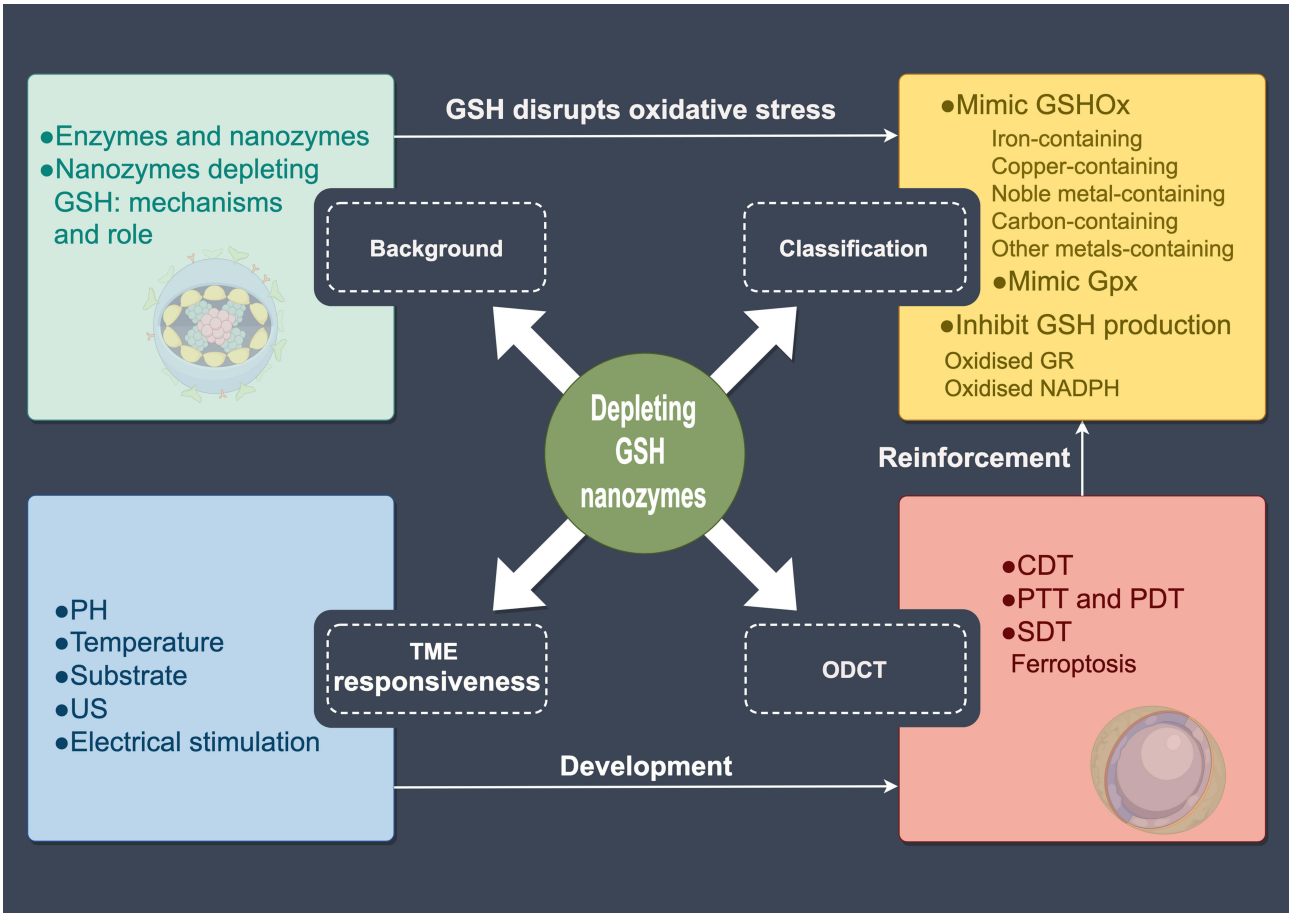

Figure 1 Article Structure. (By Figdraw) Four aspects of GSH-depleting nanozymes are presented: background, classification, TME responsiveness, and ODCT.

Table 1 Advantages and Challenges of Natural Enzymes and Nanozymes

	Nanozymes	Natural Enzyme
Advantages	Simple to synthesise.	High catalytic specificity.
	Nanozymes are mostly made of inorganic materials and are low cost.	High catalytic activity.
	Nanozymes have a larger specific surface area and are easier to modify.	High biosafety, natural enzymes are derived from plants and animals, and their safety has been proven in long-term applications.
	Ease of mass production.	Natural enzymes are now more widely used in practical applications in a variety of fields.
	Stable and easy to store.	
	Some of the nanozymes showed even higher catalytic activity in high-temperature and acidic environments.	
	Versatility, the same Nps can mimic multiple enzyme activities at the same time, which may react in a cascade to enhance the functionality of the nanozymes.	
	Easily regulated, enzyme activity can be regulated in vitro by US, NIR, magnetic field and electric current.	
	High durability, retains its enzymatic activity after many uses.	
	Unique physicochemical characteristics such as fluorescence and conductivity.	
Challenges	Most have lower catalytic activity than natural enzymes.	Prone to denaturation and inactivation.
	Low substrate selectivity, which may affect effectiveness.In the biomedical field they may even cause toxic side effects.	Most of them need to be extracted from plants and animals, which is complicated and costly to prepare.
	Safety not yet proven, possible long-term toxicity.	Limited production and difficulty in obtaining large quantities.
	The mechanism of nanozymes is still unclear.	High storage requirements make long-term storage difficult.
	Nanozymes are limited in variety and mostly confined to the study of oxidoreductase and hydrolase activities.	Requires more stringent reaction conditions and is difficult to use at high temperatures or in extreme environments such as strong acids or bases.

substances, resulting in robust antibacterial activity.[42,43] They are also utilised in biosensors for the rapid and dependable detection of a range of illnesses.[44–46] In recent years, there has been extensive research on nanomaterials that mimic biological enzymes, such as CAT, OXD and POD (Figure 2). These nanozymes have shown promise in cancer therapy by enhancing intracellular biochemical reactions, accelerating ROS production, inducing cellular oxidative damage within hypoxic tumor tissues, and enabling effective cancer therapy.[47–52]

Analyzed from the point of view of regulating ROS, nanozymes can be classified into antioxidant and pro-oxidant categories[53,54] (Table 2). Regarding pro-oxidation, nanoparticles elevate intracellular ROS levels by mimicking OXD, POD, or maintain intracellular ROS levels by consuming GSH by mimicking GSHOx, GPx. On the one hand, Iron-Based, Copper-Based, Based on Noble Metal, Carbon-based, and Vanadium-based nanoparticles have been shown to have POD-like activity to catalyze the generation of ROS from H_2O_2.[55] Fe_3O_4NPs can simulate POD to produce Fenton reaction.[56] Copper-based nanoparticles have also been reported to have the ability to mimic POD.[57] Siddiqi et al[58] demonstrated that some noble metal-based NPs exhibit excellent antimicrobial properties even at low concentrations. NC@Gox NPs generated by Xu et al[59] mimicked the POD activity to decompose H_2O_2 to produce ROS. Tian et al[60] found that the VO_2NPs possessed a POD-like activity and could be used for glucose colorimetric determination of glucose with good detection range and accuracy. On the other

https://doi.org/10.2147/IJN.S515734

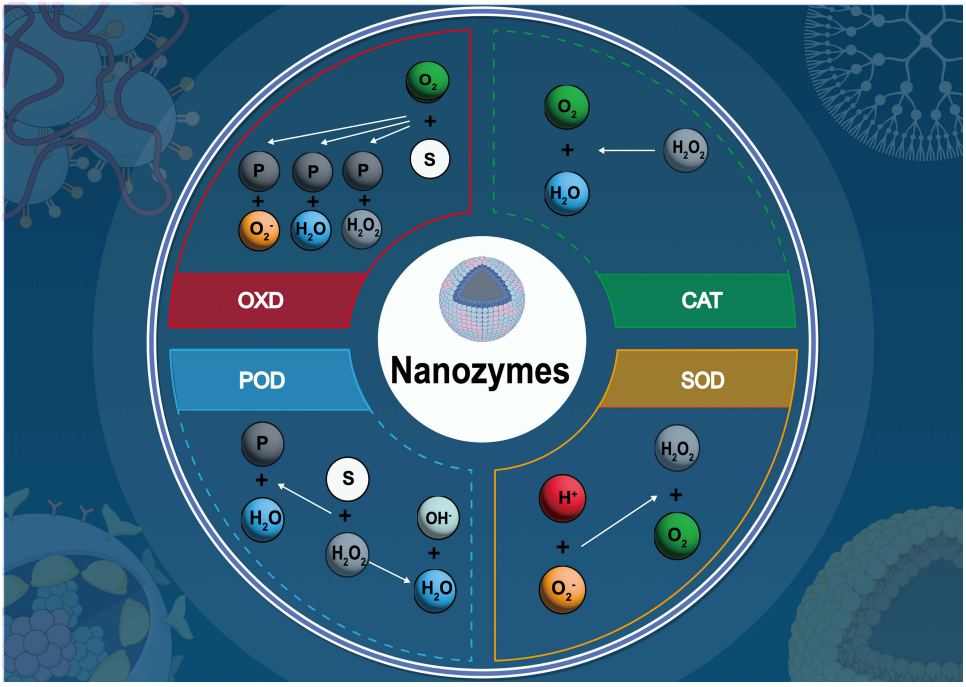

Figure 2 Catalytic schematic of nanozymes mimicking OXD, POD, SOD, CAT. (By Figdraw) Where S represents the substrate and P represents the product.

hand, the maintenance of ROS levels by mimicking GSHOx and GPx to consumption of GSH also plays a role in promoting oxidation during nanoparticle antitumor studies. Some copper-based NPs were shown to have the ability to mimic GSHOx, and the consumption of GSH levels by these NPs and synergistically with their POD-like enzyme activities jointly maintained the

Table 2 Pro-Oxidant and Antioxidant Nanozymes

Function	Nanozymes	Subtypes	Features	References
Promoting oxidation	POD-like activity	Iron-Based	Fe_3O_4NPs have both magnetic and photothermal properties and were first found to have POD-like activity.	[56]
		Copper-Based	Cu_{2-x}SeNPs have excellent photothermal conversion and anti-tumor effects. Cu_2-xTeNPs possess potent intrinsic bactericidal activity.	[57]
		Based on Noble Metal	Some based on noble metal NPs exhibit excellent antibacterial properties even at low concentrations.	[58]
		Carbon-based	The intrinsic POD-like activity of NC@Gox NPs breaks down H_2O_2 to produce ROS.	[59]
		Vanadium-based	VO_2NPs can be used for the colorimetric determination of glucose due to their POD-like activity, which has good detection range and accuracy.	[60]
	GSH oxidase-like activity	Copper-Based	The copper-based NPs possessed two biological enzyme activities similar to GSH oxidase-like and POD-like. These two enzyme activities cooperate to maintain the oxidative stress state of tumor cells.	[61,62]
Antioxidant	CAT-like activity	Cerium-based	Scavenging ROS can protect cardiomyocytes in vitro.	[63]
	SOD-like activity	Carbon-based	Carbon-based NPs reduce intracellular ROS levels through disproportionation reactions. In addition, GO has been found to function as a hydrolase.	[64]
		Melanin-based	Melanin-based unique antioxidant and anti-inflammatory effects contribute to the protection of ischemic brain.	[65]

intracellular oxidation levels in tumor cells.[61,62] Regarding antioxidants, nanoparticles reduce oxidation levels by mimicking the functions of SOD and CAT. Nanoparticles mimic CAT to catalyze the decomposition of H_2O_2 into O_2 and water, preventing oxidation. Ceria nanoparticles prepared by Ni et al[63] mimicked the activities of CAT and SOD to scavenge ROS, which were protective against cardiomyocytes in vitro. The SOD-mimicking nanozymes catalyzed the disproportionation of superoxide anion radicals to H_2O_2 and O_2. Carbon-based NPs reduced intracellular ROS levels through the disproportionation reaction.[64] The unique antioxidant and anti-inflammatory effects of melanin-based nanoparticles help protect ischemic brains.[65] This review focuses primarily on nanomaterials depleting GSH (mimicking GSHOx, GPx, OXD) for cancer therapy and discusses in detail recent advances and future perspectives.

Nanozymes Depleting Glutathione: Mechanisms and Role

GSH acts as an antioxidant and free radical scavenger and plays a critical role in several metabolic and physiological processes in the body, protecting cells from oxidative damage and damaging exogenous agents. It is involved in cell proliferation, division, differentiation and is the most commonly elevated metabolite during cellular oxidative stress.[66–69] Regarding cancer, high GSH expression is a key feature that distinguishes tumor tissue cells from normal tissue cells, which contain 8 to 10 times more GSH than normal cells.[70] On the one hand, cerium oxide Nps protects cells and tissues from oxidative stress-induced damage due to its self-regenerating redox cycle. Singh et al[71] further demonstrated the use of pegylated cerium oxide Nps as an effective pharmacological agent for the treatment of free radical mediated diseases at low GSH/GSSG ratios. On the other hand, many studies have shown that nanozymes improve the efficacy of ROS-based ODCT, radiotherapy, chemotherapy, and immunotherapy by mediating the depletion of GSH, which makes cancer cells more susceptible to oxidative stress. As previously mentioned, scholars have made significant efforts to develop strategies that effectively deplete GSH using nanozymes that mimic GSHOx, GPx and OXD.

Currently, there are two main strategies for depleting tumor GSH using nanozymes. The first involves mimicking GSHOx or GPx to downregulate extant GSH levels in tumour cells. After co-incubation of GSHOx or GPx mimicking nanozymes with GSH, 5.5′-dithiobis (2-nitrobenzoic acid) (DTNB) was used as a probe to detect the -SH group in GSH. The results showed that GSH was clearly reduced by analysing the UV-visible signal obtained from the resulting yellow product (5-Thio-2-nitrobenzoic acid(TNB)) at 412 nm[72–74] (Figure 3).The second involves partial mimicking OXD

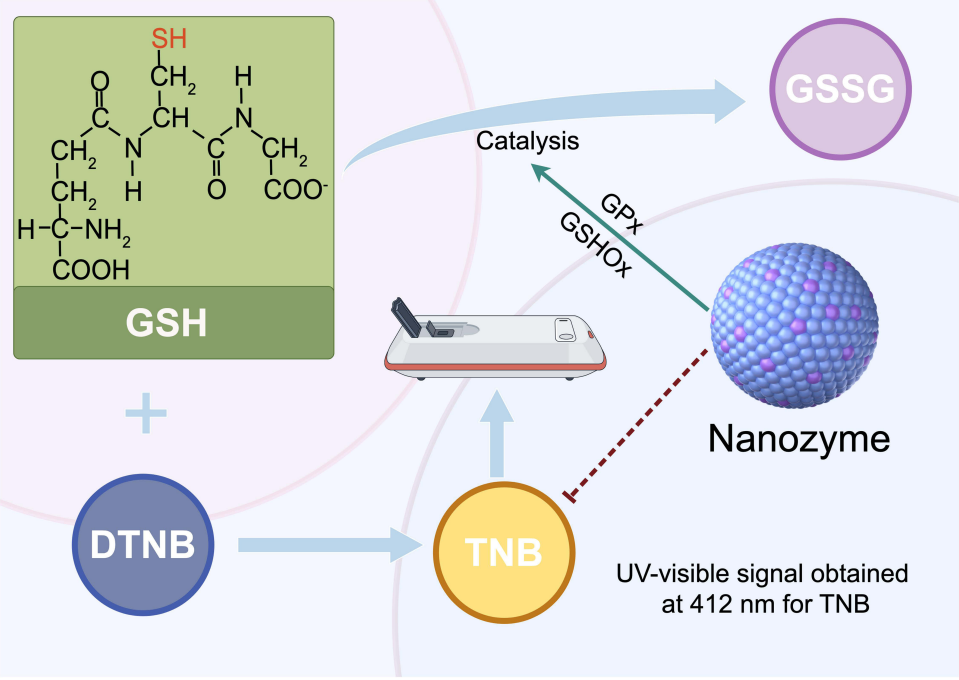

Figure 3 Principle of GSH Detection by DTNB. (By Figdraw).

https://doi.org/10.2147/IJN.S515734

nanozymes, which impede GSH production. They interfere with the reduction of GSSG to GSH by oxidising glutathione reductase (GR) or the coenzyme of GR (reduced nicotinamide adenine dinucleotide phosphate (NADPH)).[75,76] Nanozymes have considerable advantages over enzymes for inducing GSH depletion, including high stability, low cost, tunability and easy multifunctionalisation. This makes them potential candidates for biomedical applications, particularly in cancer therapy. This review will focus on the biomedical applications of nanozymes depleting glutathione.

Classification of Nanozymes Depleting Glutathione

Nanomaterials with multiple enzymatic activities, including GSHOx, GPx, OXD, POD, and CAT, have been developed by scientists to increase intracellular ROS levels through enzymatic cascade reactions.[77,78] This section will focus on nanomaterials that imitate GSHOx, GPx, and OXD (oxidized GR and NADPH) to reduce GSH levels. The discussion of the 'explosion' of ROS generated by multiple enzyme cascades will be presented in section 6.

Mimic Glutathione Oxidase

In tumor cells, the high concentration of GSH (≈10×10^{-3}M) greatly limits the effectiveness of nanozymes in treating tumors.[79] Nanomaterials exhibiting GSHOx-like catalytic activity facilitate the oxidation of GSH to GSSG and the reduction of O_2 to H_2O_2.[80] The reaction equation is: $GSH + O_2 \rightarrow GSSG + H_2O_2$. During this process, O_2 is reduced to generate reactive products such as ROS, including superoxide anion radicals ($-O^-_2$) and H_2O_2. Additionally, the depletion of GSH weakens the resistance of tumor cells to oxidative stress, making them more susceptible to ROS damage.[80,81] This subsection presents a classification of nanomaterials according to the elements that may confer GSHOx activity to them. This classification is presented in five categories: NPs containing iron, copper, noble metals, carbon and other metallic elements. The GSHOx mimicking behavior and GSH depletion mechanisms of these NPs are presented.

Iron-Containing

Spherical pyrite (FeS_2) NPs with the ability to mimic GSHOx have been reported by Fan et al.[72] After incubation of FeS_2NPs with GSH at concentrations of 0.1,0.3 and 0.5 mg/mL, respectively, the absorbance of TNB produced by the reaction of DTNB with GSH showed a dose and time dependent decrease in absorbance at 412 nm. Furthermore, GSH depletion was enhanced in the oxygen (O_2) environment and inhibited in the nitrogen (N_2) environment. It is further shown that FeS_2 mimics GSHOx to oxidise GSH and consume O_2 to generate H_2O_2, providing sufficient raw material for ROS generation. Huang et al[82] conducted a study in which they encapsulated FeS_2NPs and the chemotherapeutic drug camptothecin into an injectable hydrogel. They achieved photoreactive controlled release of FeS_2 and camptothecin under the photothermal effect mediated by near infrared light (NIR) at 0.5 W/cm^2. In a separate report, Liu et al[83] created FeS_2 biomimetic nanozymes by enclosing FeS_2NPs in exosomes derived from cancer cells. This resulted in an extended blood circulation time of FeS_2 in vivo. Additionally, FeS_2 was engineered to possess immune evasion capabilities and homologous targeting towards tumor tissues, thereby enhancing its biological potential for application.

Heterogeneous diatomic site nanozymes utilize two different metal atoms in close proximity to achieve functional complementarity and synergy. They can modulate the energy barriers of reaction intermediates through electron interaction between the two neighboring heterogeneous metals.[84] Scholars have developed iron-containing heterogeneous nanozymes with two-atom sites to accelerate the depletion of GSH in tumor cells. Chen et al[85] designed a Mn/Fe diatomic nanozyme (DAzyme) with satisfactory GSH consuming ability by coordinating Mn/Fe atoms to nitrogen atoms in hollow zeolitic imidazolate framework (ZIF). X-ray photoelectron spectroscopy (XPS) confirmed the dual active sites of Mn and Fe in Mn/Fe DAzyme. Zhang and colleagues[86] produced FeCo/Fe-Co DAzyme by etching N-doped graphene-encapsulated FeCo nanocages with sulfuric acid at 80°C. Aberration-corrected high angle annular darkfield scanning transmission electron microscopy (HAADF-STEM) clearly revealed the dispersed atomic metal sites on the shell of N-doped graphene. Co-incubation of 4T1 cells with 50 μg/mL of FeCo/Fe-Co DAzyme depleted almost 57% of intracellular GSH without causing any toxicity. The recent study by Lu et al[87] showcased the impressive GSHOx catalytic activity of covalent organic framework $COF_{FePc\ (quasi\text{-}iron\ phthalocyanine)}$ nanosheets. The Michaelis Menton kinetics of GSH catalyzed by COF_{FePc} indicate that the calculated values of K_m and V_{max} were 9.78×10^{-3} M and 8.17×10^{-5} M/S, respectively. These values were found to be significantly higher than those of other iron-containing nanozymes (V_{max} (COF_{FePc}) ≈ 80 V_{max} (FeS_2 or FeCo/Fe-Co)) (Table 3). Upon internalisation into 4T1 cells, COF_{FePc} is released

Table 3 Depletion of GSH Nanozymes Mimics Vmax and Km for GSHOx, GPx, POD, OXD, and CAT

Depleting GSH Nanozymes Formulation	Mimic Enzyme Activity	Substrate	V_{max}(M/s)	K_m(mM)	References
FeS_2	GSHOx	GSH	9.8×10^{-7}	0.66	[72]
(BSA)-Ce6&NO-RuO_2	CAT	H_2O_2	3.967×10^{-5}	3.66	[75]
	GPx	H_2O_2	7.883×10^{-7}	1.8	
		GSH	1.103×10^{-6}	90.2	
FeCo/Fe-Co	GSHOx	GSH	1.07×10^{-6}	1.775	[86]
	OXD	TMB	1.833×10^{-7}	0.47	
	POD	H_2O_2	2.811×10^{-7}	0.845	
COF_{FePc}	POD	H_2O_2	1.35×10^{-6}	3.036	[87]
		TMB	4.3×10^{-6}	1.06	
	GSHOx	GSH	8.17×10^{-5}	9.78	
PEG-Cu_2WS_4	POD	H_2O_2	3.8×10^{-3}	1250	[88]
	GSHOx	GSH	3.2×10^{-5}	1.28	
Cu_2O	GSHOx	GSH	16.16×10^{-6}	0.47	[89]
	POD	H_2O_2	6.86×10^{-8}	0.301	
$Mn_3Cu_3O_8$	GSHOx	GSH	8.85×10^{-6}	0.287	
	POD	H_2O_2	3.09×10^{-7}	0.231	
$Cu_2O@Mn_3Cu_3O_8$	GSHOx	GSH	14.95×10^{-6}	0.436	
	POD	H_2O_2	1.013×10^{-7}	0.112	

into the cytoplasm due to lysosomal dysfunction. It consumed over 85% of GSH at a concentration of only 30ug/mL. When combined with NIR, this consumption increased to over 90%.

Scholars have also explored the mechanism of iron-containing NPs that mimic GSHOx. Hu et al[90] prepared Co-$FeSe_2$ nanoflowers using a simple thermal injection method. After 4 hours, the conversion of GSH catalyzed by Co-$FeSe_2$ reached 70%. This was due to the consumption of GSH by oxidising Fe^{3+}/Co^{3+} ions and Se-Se bonds. Wang et al[91] prepared Co/La-Prussian blue (PB) nanozymes that exhibit GSHOx activity. The authors confirmed the reaction mechanism of GSH depletion by verifying the change in Co/La-PB valence before and after the reaction using XPS. Following the reaction, the peak at 711.6 eV was notably weakened, indicating the reduction of some Fe^{3+} to Fe^{2+}. Similarly, the peak area at 781.7 eV, representing Co^{2+}, increased, providing evidence that some Co^{3+} was reduced to Co^{2+}. These results suggest that metal ions (Co^{3+} and Fe^{3+}) in the high oxidation state act as oxidants and deplete GSH in the cells. Chiang et al[92] prepared Fe^{3+} coordinated nanozymes using Fe^{3+}/Fe^{2+} as a redox coupling agent to effectively deplete GSH. Lin et al[93] similarly demonstrated this, the redox pairs (Fe^{3+}/Fe^{2+}) of GSH were 2.08 and 1.57 before and after incubation with their prepared nanozymes, resp.

Copper-Containing

Copper-based NPs were also used as GSHOx analogues. Ye et al[94] synthesised $Cu_{2-x}Se$ NPs with GSHOx mimicking activity at room temperature via an ascorbic acid reduction reaction, which impairs intracellular antioxidant regulation by depleting overexpressed GSH. Zhao et al[73] prepared polyethylene glycol@$Cu_{2-x}S$@Ce6 nanozymes (PCCN) using a one-step hydrothermal method. The redox pair of Cu^+/Cu^{2+} in PCCN has great potential for oxidizing GSH. The high-valent Cu^{2+} with oxidative capacity catalyzes the production of GSSG from GSH. As the concentration of PCCN increases, the

https://doi.org/10.2147/IJN.S515734

amount of GSH progressively decreases. The intracellular depletion of GSH was assessed, and it was found that 150ug/mL of PCCN consumed almost 60% of the GSH in 4T1 cells. Hao et al[88] synthesized a nanozyme called polyethylene glycol-modified Cu_2WS_4 (CWP) using the sacrificing template method. The enzymatic kinetics of GSH oxidation catalysed by CWP, which simulated GSHOx, were further investigated. The V_{max} and K_m values were found to be 3.2×10^{-5} M/S and 1.28×10^{-3}M, respectively. Co-incubation of CWP at a concentration of 20 μg/mL with 4T1 cells resulted in a 25% reduction in intracellular GSH content.

Hou et al[89] prepared a core-shell-structured nanozyme, $Cu_2O@Mn_3Cu_3O_8$ (CMCO). The shell of $Mn_3Cu_3O_8$ prevents normal tissues from being exposed to the Cu_2O core until it reaches the tumor lesion, reducing systemic toxicity. Furthermore, $Mn_3Cu_3O_8$ has an enhanced electron-hoarding capacity and a d-band center closer to the Fermi level, making it a potential mimic of GSHOx. DTNB was used as a probe to detect CMCO depletion of GSH. The V_{max} and K_m values were 14.95×10^{-6} M/S and 4.36×10^{-4} M, respectively. After treatment, CMCO reacts with H_2S in an acidic environment and decomposes into Cu ions, Mn ions, and ultra-small Cu7S4 NPs. These NPs can be efficiently excreted from the body in the urine through the renal filtration system, preventing the long-term retention of inorganic NPs in the body.

Due to the unique chemical reaction activity of the element copper, atomic copper active sites are present in many natural enzymes, such as cytochrome C oxidase and SOD, which are involved in important biochemical processes.[95] Therefore, the depletion of GSH by artificial Cu single atom nanozyme (SAzyme) for catalytic antitumor therapy has gained attention. In 2021, Cheng et al[96] constructed Cu single atom sites/N-doped porous carbon nanozymes and demonstrated the consumption of GSH by Cu SAzyme. Recently, Lin et al[97] have constructed a Cu-nanotransformer using a Cu^{2+}/phloretin co-loaded disulfide bond (S-S) bridged dendritic mesoporous organosilica(DMSN) NPs skeleton. Upon internalization of the Cu-nanotransformer by CT26 cells from BALB/c mice, the overexpressed GSH reacted with S-S, leading to the collapse of the backbone of DMSN NPs. This resulted in the release of loaded phloretin and adsorbed copper ions. Cu ions that were not released were immobilized by Si-OH to form a Cu SAzyme. This enzyme contains $Cu\text{-}O_4$ and $Cu\text{-}O_2$ atomic centers that have high spatial distribution and atomic stability, which consumed nearly 30% of intracellular GSH. Na et al[98] prepared dual single-atom ultrathin 2D metal organic framework (MOF) NSs (Pd/Cu SAzyme). After 3 hours, Pd/Cu SAzyme at a concentration of 200ug/mL consumed 60% of GSH. After 12 hours, more than 90% of GSH was consumed. In addition, they explored the mechanism of GSH depletion, which is based on Cu^{2+} mediated oxidation of GSH to produce the GSCuSG complex. When Cu^{2+} binds to -SH, it is reduced to Cu^{+} and forms the intermediate Cu^{+} (SG). ·GS then splits from another GSH molecule and reacts with Cu^{+} (SG) to facilitate the formation of GSCuSG, completing the process of GSH oxidation. It is also well illustrated that the ability of copper-containing NPs to mimic GSHOx is closely related to the redox pair Cu^{+}/Cu^{2+}.

Noble Metal-Containing

The noble metal material has excellent catalytic activity. NPs made from it have a greatly increased specific surface area and abundant dangling bonds, making them more promising catalysts for applications.[99–101] Currently, noble metal NPs and nanoframes loaded with noble metals have successfully mimicked GSHOx. This section focuses on the depletion of three noble metal materials, Au, Pt and Pd, for GSH. Liu and colleagues[102] prepared Au-Cu^{2+}-ZIF-DOX (ACD) nanozymes by encapsulating Au nanoclusters (NCs) and DOX into Cu^{2+}-doped ZIF-8 shells. After incubation of Au NCs with GSH, the absorbance at 412 nm gradually decreased to 78.6% after 3h, 41% after 24h and 18.5% after 48h. This decrease in absorption favours the CDT of tumors. Chang et al[103] prepared Bi_2Te_3 NCs loaded with Au/Pd bimetallic NPs, named BAP NCs. The consumption of GSH significantly increased with the concentration of BAP NCs (0–120 μg/mL) and the reaction time (0–5 min). Following incubation with BAP NCs, the relative GSH levels in 4T1 cells decreased significantly by 60%. Ye et al[104] prepared a super-stable metallo-supramolecular nanoassembly (FPIC) based on amino acids, driven by Pt^{4+}, using a simple reprecipitation method. In the presence of GSH, the absorbance of DTNB at 412 nm decreased as the concentration of Pt ions in FPIC NPs increased. After co-incubating FPIC NPs with 4T1 cells for 12 hours, the GSH/GSSG ratio decreased from 100% to 50%.

To enhance the catalytic performance, Gong et al[105] constructed a novel nanocomponent (carbon dots (CDs)@Pt single atoms (SAs)/NCs@DOX) with 34.8% platinum loading. The K_m and V_{max} of CDs@Pt SAs /NCs in the catalytic reaction of GSH were 1.04 mm and 7.46×10-6 M/s, respectively, which were comparable to those reported for GSHOx-

like nanozymes. The XPS results indicate that the content of Pt^{0+} increased from 23.4% to 41.24% after the reaction of CDs@Pt SAs/NCs with GSH. This suggests that Pt^{2+} was reduced to Pt^{0+} to complete the oxidation of GSH.

After the addition of GSH, the fluorescence quantum yield of CDs@Pt SAs/NCs changed from 3.05% to 5.8%, which was lower than that of CDs, which could be due to only a small part of the Pt^{0+} shedding exposing some of the N atoms present on the surface of CDs@Pt SAs/NCs. It is suggested that CDs@Pt SAs/NCs exhibit remarkable catalytic properties, probably due to the fact that most of the Pt SAzyme/NCs are retained as active sites on the CD surface. Recently, Xu et al[106] designed a bimetallic ion-modified MOF nanozymes (Zr^{4+}-MOF-Ru^{3+}/Pt^{4+}-Ce6@HA, ZMRPC@HA) for long-term catalytic therapy of tumors. The experimental results indicate that although the ZM skeleton nanomaterials adsorbed GSH on their own, only 21% of GSH was removed after 6h. In contrast, the introduction of Pt^{4+} into ZM greatly increased the GSHOx activity of the nanomaterials. At a ZMP concentration of 200 μ/mL, the GSH consumption rate reached 56% within 30min and ultimately 85% after 120min of reaction. ZMRPC@HA dispersed in a simulated TME solution containing 100 μM H_2O_2 and 2mM GSH maintained a 71.8% depletion of GSH after three days, which is expected to be a long-term and stable GSH depletion strategy in tumor therapy.

Carbon-Containing

Dugan et al[107] first suggested that carbon nanomaterials have enzyme-like activity. They found that fullerene derivatives can act as SOD mimics, scavenging -O^{-}_{2}. In recent years, scholars have begun to explore the depletion of GSH by carbon-based nanomaterials such as carbon nanotubes, CDs, and graphene oxides (GOs) as a potential strategy for tumour therapy. This section discusses carbon nanotubes and CDs that mimic GSHOx. GOs mimicking GPx will be discussed in 4.2. Soheila et al[108] discovered that both single-walled carbon nanotubes and multi-walled carbon nanotubes can down-regulate GSH, leading to an increase in cellular oxidative stress. Yousef et al[109] further observed a significant decrease in intracellular GSH levels in mice exposed to carbon nanotubes in animal experiments. Zeng et al[110] reported a biocompatible nanozyme based on chlorogenic acid (ChA) doped CDs. The ChA CDs (100 μg/mL) were treated with different concentrations of GSH in the presence of DTNB. The absorbance of GSH at 422 nm decreased with increasing time and GSH concentration, indicating effective removal of GSH by the ChA CDs. Recently, Luo et al[111] prepared CDs-based nanosystems modified by poly-ethylenimine, carrying siRNA and DOX, which exhibited GSHOx activity. Co-incubation of CD-poly-ethylenimine (200 μg/mL) with GSH showed a time- and concentration-dependent depletion of GSH.

Heteroatom doping can effectively enhance the catalytic activity of catalysts by optimizing the electronic structure of the active sites in carbon materials.[112] Shen et al[113] have developed a new nanoplatform called Pt/N-CD@TiO_{2-x}, which incorporates N-doped CDs and can be used for both detecting and depleting GSH. With regard to the detection of GSH, when N-CDs and Pt/N-CD NPs were incubated with LO2 cells (GSH, 0.36±0.04 mm), HeLa cells (GSH, 2.23 ±0.15 mm), and 143B cells (GSH, 2.54±0.23 mm), respectively, there was a notable absence of fluorescence contrast between the three groups of cells in the presence of N-CDs. In contrast, high fluorescence contrast was observed for Pt/N-CD NPs with 143B cells and HeLa cells after 6 h of incubation. With regard to glutathione (GSH) depletion, no significant depletion was observed in the pristine N-CD. In contrast, the characteristic absorbance peak of DTNB (412 nm) of Pt/N-CD NPs exhibited a sharp decrease with increasing incubation time, indicating that GSH depletion by Pt/N-CDs was occurring. Wang et al[64] doped MnO into mesoporous carbon (MC) to create a smart MC nanoplatform (CCM). The CCM was able to consume nearly 70% of GSH after co-incubation with 4T1 cells and maintain low intracellular GSH levels for 24 hours, demonstrating an efficient and long-lasting GSH consumption ability. The catalytic reaction rate of CCM was slightly lower under hypoxic conditions than under normoxic conditions by about 70%, further suggesting that CCM mimics the behaviour of GSHOx. Zhang et al[114] constructed Fe^{3+}-modified l-histidine-sourced CDs (FeCDs). The GSH/GSSG ratios of the groups subjected to oxidative stress control, CD treatment, or FeCDs treatment were approximately 85%, 60%, and 30%, respectively. The statement suggests that CDs are capable of consuming GSH, and the presence of Fe^{3+} enhances this ability, resulting in the dual consumption of GSH. It is evident that carbon-based nanoenzymes have the capability to imitate GSHOx and can also serve as effective carriers for constructing multi-functional nanoplatforms.

Metal-Organic Frameworks

Metal-Organic Frameworks (MOFs) are a class of porous crystalline materials formed by self-assembly of metal ions/clusters with organic ligands via coordination bonds. In recent years, MOFs have been widely explored as biomimetic platforms for Nanozymes due to their modifiability, high specific surface area, and structural tunability, providing innovative strategies for efficient catalysis, biosensing, and disease treatment.[115] Wang et al[116] created a bimetallic nano-enzyme system ZIF-8/SrSe derived from MOF and encapsulated with DOX enzyme kinetic analyses showed that the nanozyme exhibited substantial GSHOx-like activity and efficiently oxidized reduced GSH to GSSG. Furthermore, ZIF-8/SrSe@DOX nanoparticles efficiently transported DOX, which caused DNA damage and further promoted apoptosis and Ferroptosis. Lin et al[93] fabricated a biocatalytic Janus nanocomposite based on an iron-zirconium porphyrin metal-organic framework [PCN-224(Fe)] for ultrasound-driven SDT and 808 nm NIR light-mediated PDT. ROS production was facilitated by GSH consumption and oxygen supply. Recently, a nanoplatform synthesized by Tu et al[117] by embedding a monovalent Au nanozyme into a photosensitive MOF structure using an in situ redox method effectively depleted existing GSH, thereby improving the efficacy of PDT and PTT. Wu et al[118] designed MOF-based nanoplatforms that similarly oxidized GSH to GSSH.

Containing Other Metal Elements

Nanomaterials that contain other metals, such as Mn, vanadium (V), bismuth (Bi), and cobalt (Co), were also successfully used to simulate GSHOx. Gang et al[119] prepared a nanoplatform with mesoporous silica NPs as the core and MnO_2 as the shell. This platform markedly reduced GSH levels in 4T1 cells. Xu et al[120] constructed a bimetallic nanoplatform with atomically dispersed Mn/gadolinium (Gd) double sites by hydrothermal method, which also exhibited efficient consumption of GSH. Additionally, the Gd sites modulated the local electrons of the atomically catalyzed Mn sites, thereby enhancing the GSHOx activity of the nanoplatform. Bai et al[121] prepared nanozymes composed of hydroxyapatite and $CuMnO_x$, and verified the mechanism of GSH depletion. Hydroxyapatite-$CuMnO_x$ was dispersed in phosphate buffer with or without the addition of GSH and the release of Mn was determined at different times. The oxidation of GSH resulted in a gradual decrease in the ratio of Mn^{4+}/Mn^{2+} in solution, indicating that Mn^{4+} oxidised GSH to produce Mn^{2+}. Hao et al[122] conducted experiments that demonstrated the depletion of GSH by high-valence Mn ions. They designed bismuth-Mn-shell nanoflowers containing glucose oxides for GSH depletion in 4T1 tumors. In this case, the reduction potential of Mn^{3+} to Mn^{2+} was found to be similar to the oxidation potential of GSH to GSSG, indicating a possible correlation between the oxidation of GSH and Mn^{3+}/Mn^{2+}. XPS results revealed that after treatment with 2mM GSH for 4h, the valence state of Mn consisted of 38.3% Mn^{3+} and 61.7% Mn^{2+}, suggesting that Mn^{3+} conferred the nanomaterial with the ability to mimic GSHOx. The presence of Mn was almost undetectable in the 10 mm GSH-treated solution, indicating that the high concentration of GSH had been completely consumed by Mn^{3+}.

Vanadium has multiple valence states, with the most common being V^{4+} and 0.5+[123] The enzymatic activity of V-containing nanomaterials is affected by the different valence states. Li et al[124] synthesized four vanadium oxide nanozymes (Vnps) using a simple method. The Vnps included Vnps-I, which consisted of pure V^{5+}; Vnps-II, which consisted of mixed V^{5+}/V^{4+}; and Vnps-III and Vnps-IV, which consisted of V^{4+}. Vnps-III was found to consume significantly more GSH than the other three nanozymes at all concentrations. Co-incubation of only 10ug/mL of Vnps-III with 4T1 cells resulted in the consumption of nearly 85% of the intracellular GSH. Recently, Yang et al[125] developed a new nanoplatform ($ZnSnO_3$@MXene) by loading ultra-small $ZnSnO_3$ NPs onto MXene, a V-containing V_2CTx NCs. The $ZnSnO_3$@MXene nanoplatform showed a time-dependent depletion of GSH when DTNB was used as a probe. The V^{4+} produced by $ZnSnO_3$@MXene was converted to V^{3+} with POD-mimicking ability by oxidising GSH, achieving a dual enzyme-catalysed cycle of GSHOx and POD. Li et al[126] fabricated Bi NCs (Bi-N/C) on nitrogen-doped porous carbon. The absorbance at 412 nm decreased as the concentration of Bi-N/C increased, indicating that Bi-N/C could potentially mimic GSHOx. Using a simple sacrificial template method, Lin et al[127] synthesized Co single atom-supported N-doped carbon nanozymes (Co SA-N/C). The introduction of Co atoms greatly down-regulated the GSH level, as evidenced by the significant decrease in absorbance at 412 nm when compared to SA-N/C. Furthermore, it has been discovered that nanomaterials containing molybdenum,[128] nickel,[129] and cerium [20] can imitate GSHOx. The above demonstrates the potential of nanozymes containing high valence metal ions in mimicking GSHOx (Figure 4).

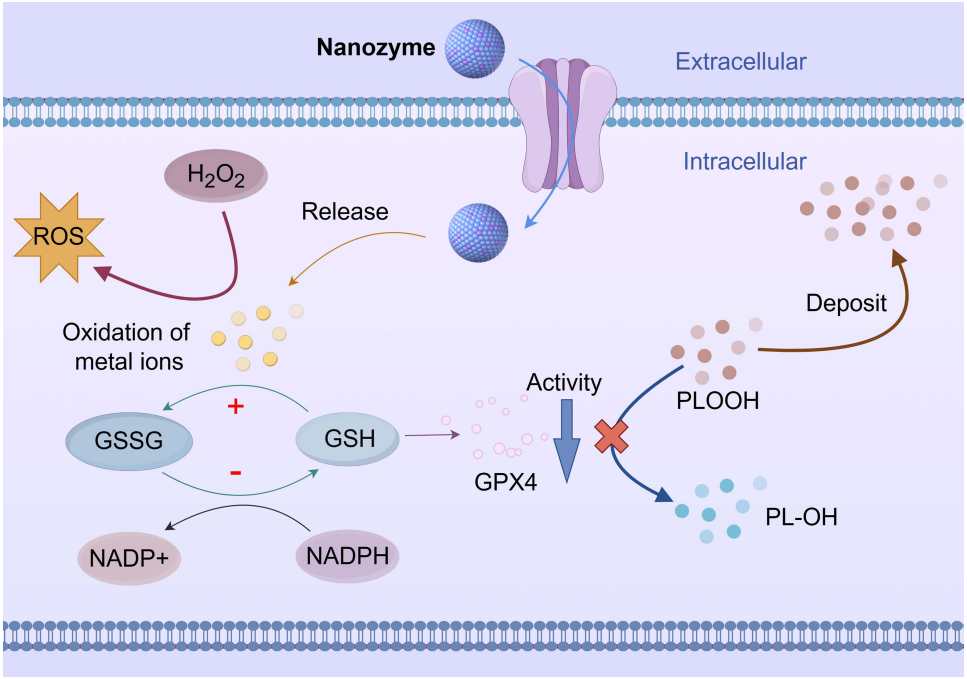

Figure 4 The nanozymes release metal ions, causing GSH depletion as well as ROS accumulation. (By Figdraw).

Mimic Glutathione Peroxidase

It is well established that natural GPx is a peroxide disintegrating enzyme that is widely distributed throughout the organism. It oxidises GSH to GSSG, thereby reducing toxic peroxides to non-toxic hydroxyl compounds. Concurrently, it catalyses the decomposition of H_2O_2, thus protecting the structure and function of the cell membrane from the interference and damage of peroxides.[68,130] The reaction equation is: GSH + H_2O_2 → GSSG + H_2O. Synthetic NPs that mimic GPx compete with natural GPx for inhibition, thereby weakening the protective effect of natural GPx on tumor cells. This subsection will introduce 6 NPs that mimic GPx.

Yang et al[74] designed an ultrasmall bimetallic oxide nanozyme, $CuFe_2O_4$ NPs, which was shown to possess GPx activity. The nanozyme was mixed with GSH and the UV-visible signal of -SH in GSH at 412 nm was detected using DTNB as a probe. The results demonstrated a significant depletion of GSH within six hours. Zhao et al[131] prepared polyethylene glycolated MC (MC-PEG) as a carrier for indocyanine green and compared it with polyethylene glycolated GOs (GO-PEG). The consumption of 10 mm GSH by 200 μg/mL of MC-PEG was almost complete within 10 h, resulting in a solution of 6-nitro-m-toluic acid that changed from yellow to almost colorless. In contrast, the color of the GSH/GO-PEG solution remained largely unchanged, indicating that MC-PEG exhibits an exceptional ability to consume GSH. At the cellular level, naphthalene-2,3-dicarboxaldehyde was employed as a sulfhydryl tracer for labelling intracellular GSH. Following a 8 hour co-incubation period with GO-PEG, there was no discernible change in GSH levels in 4T1 cells. In contrast, the green fluorescence in 4T1 cells was diminished after 4 h of incubation with MC-PEG, and almost completely extinguished after 8 h. Zhu et al[132] synthesized amorphous $CoSnO_3$ nanocubes with efficient GPx-like catalytic activity. The decrease in DTNB absorbance at 412 nm with increasing incubation time demonstrated the effective consumption of GSH by $CoSnO_3$, which may be attributed to the Sn^{4+}-mediated GPx-like activity of $CoSnO_3$. The content of GSH in tumor tissues of mice following different treatments was further examined. The GSH/GSSG ratios (less than 25%) of the $CoSnO_3$ group and $CoSnO_3$ combined with NIR were found to be significantly lower than those of the control group and the NIR alone group. Hu et al[133] successfully mimicked GPx by synthesising PtMnIr NPs via a one-step solvothermal method. The absorbance of GSH at 412 nm decreased rapidly with time in the presence of PtMnIr. The excellent catalytic activity may be attributed to the induced asymmetric charge distribution and interactions between different metals. Specifically, Pt can regulate the adsorption of -OH on Ir species in an inverse manner, and

https://doi.org/10.2147/IJN.S515734

alloying Mn may result in a downward shift of the d-band centre of Pt, which may lead to a reduction in the strength of the bond between Pt and oxygenated species. In a study by Li et al,[134] a defect engineering strategy was employed to prepare Pt-doping MoOx (PMO) redox nanozymes with rapid degradation properties. These nanozymes were then assembled onto Poly (lactic-co-glycolic acid) (PLGA) via a microfluidics chip, thus resolving the conflict between maintaining therapeutic activity and rapid degradation. The absorbance of the DTNB solution containing PLGA@PMO and GSH decreased significantly with the reaction time. XPS spectroscopy was employed to analyze the changes in the oxidation state of Mo ions during the above-described enzyme-catalyzed process. The Mo^{6+} concentration of the untreated PMO nanozymes was 45.2%, while that of the GSH-treated nanozymes was 25.3%. This indicates that Mo^{6+}, which has oxidative potential, was involved in the GSH oxidation. In a recent study, Zhang et al[135] successfully anchored Ir NCs on Co (OH) nanosheets and prepared an Ir content of 6.2 wt% ($Ir_{6.2}$-Co (OH)). The characteristic absorption of DTNB at 420 nm was significantly diminished in solutions dispersed with both $Ir_{6.2}$-Co (OH) and $Ir_{1.4}$-Co (OH). Conversely, the characteristic absorption of DTNB in the Ir and Co (OH) groups exhibited minimal change, which could be attributed to the absence of Ir^{4+}. The potential mechanism of Ir6.2 -Co (OH) nanozymes mimicking GPx was further elucidated by XPS characterization. The ratio of Ir^{3+}/Ir^{4+} following the reaction with GSH was 1.13, representing a 1.8-fold increase from the state prior to GSH oxidation. Furthermore, no significant alterations were observed in the Co 2p and O 1s spectra. This indicates that the oxidation of GSH is primarily attributed to the shift in the valence state of the interfacial Ir-O site from Ir^{4+} to Ir^{3+}.

Mimic Oxidase

The above NPs, which mimic GSHOx and GPx, oxidize GSH to GSSG, thereby reducing the intracellular GSH level. Nevertheless, GSH can be generated de novo through alternative metabolic pathways in vivo, which may diminish the efficacy of the nanozymes in killing tumor cells. For instance, even in the absence of glucose, glutamine is converted to glutamate by glutaminase (GLS), ultimately resulting in the production of GSH.[136,137] GR catalyzes the conversion of GSSG to GSH with the involvement of NADPH.[138] Consequently, as researchers delve deeper into the subject of GSH consumption, they are increasingly turning their attention to the possibility of inhibiting GSH production in order to reduce GSH levels even further. Sun et al[21] grafted the GLS inhibitor CB839 onto the nanoparticle enzyme and blocked the glutamine pathway and GSH biosynthesis. However, in this process, it was the externally attached CB839 that played a role and did not reflect the properties of NPs mimicking enzyme catalysis. In recent studies, scholars have found that the two nanozymes that mimic OXD, downregulate GR and NADPH, respectively, thereby interfering with GSH production.

Zhong and colleagues[75] prepared a multicomponent bovine serum albumin (BSA)-Ce6&NO-RuO_2 nanozyme (BCNR). On the one hand, BCNR was observed to convert GSH to GSSG, thereby exerting GPx mimetic activity. The GSH level was found to gradually decrease with the prolongation of incubation time. The GPx-mimic activity of BCNR was investigated by independently varying the concentrations of H_2O_2 and GSH, and the catalytic performance of BCNR was studied by steady-state kinetics. The K_m and V_{max} of BCNR with H_2O_2 as substrate were 1.8 mm and 47.3 μM/min, respectively. The K_m and V_{max} values of BCNR with GSH as substrate were 90.2 mm and 66.2 μM/min, respectively. On the other hand, the generation of $ONOO^-$ under sonication stimulation resulted in a downregulation of GR and the avoidance of GSH regeneration. In a recent study, Lin et al[76] prepared a MnOx-coated Au (AMO) nanoflow as a nanozyme for NADPH oxidase, which was reported to be an effective tumor therapy. The intracellular treatment with 100ug/mL and 150 ug/mL of AMO for 10 h resulted in the consumption of more than 70% and 95% of GSH, respectively. This suggests the potential of AMO for GSHOx. Secondly, the rapid decrease in intracellular GSH levels may be partly attributed to the oxidation of NADPH by AMO. Following 10 hours of intracellular treatment with 100 μg/mL of AMO, there was a discernible decline in cellular NADPH levels in treated cells relative to untreated controls. Concurrently, cellular $NADP^+$ levels exhibited an upward trend, indicating that AMO possesses the capacity to catalyze the oxidation of NADPH to $NADP^+$. The selective inhibition of intracellular GSH production and depletion of the existing GSH through the use of a single nanoparticle may represent a novel approach to the development of anti-tumor nanozymes in the future. This approach could potentially facilitate the achievement of ROS "explosion" in tumor cells, thereby overcoming one of the major obstacles currently limiting the efficacy of such therapies.

Nanozymes Depleting Glutathione for Tumor Microenvironment Responsiveness

TME is composed of various non-epithelial cells in the tumor tissue as well as extracellular matrix. The development, growth and metastasis of tumors are closely related to the TME in which the tumor cells are located.[139,140] Malignant tumor cells are in a TME characterized by weak acidity, hypoxia and high expression of GSH and H_2O_2.[141] In order to develop GSH-depleted nanozymes as antitumor drugs, it is essential to ensure their stability within the TME. A further requirement is to design nanozymes that can respond to the TME to deplete GSH, thereby rendering the TME a favorable factor contributing to the anti-tumor activity of the nanozymes. This subsection will examine the response properties of the nanozymes of GSH-depleted to various factors, including pH, temperature, substrate concentration, and other variables (Table 4).

Table 4 Depletion of GSH by Nanozymes in Response to pH, Temperature, Substrate, Electrical Stimulation and US

Depleting GSH Nanozymes Formulation	Responsiveness	Feature	References
Au-Cu^{2+}-ZIF-DOX	PH responsiveness	Degradation of ZIF-8 under acidic conditions increased the release of DOX by up to 41.97% after 36 h.	[102]
T-BTO /MoS_2@CA		CA is PH-responsive and mediates H_2O_2 self-supply.	[128]
HA-$CuMnO_x$		Acidic conditions enhanced the activity of the nanomaterials to mimic GSHOx, which may be related to the increased release of Mn^{4+}.	[121]
Bi-DOPA@BSA-GOx@MnO_x		BDS-GOx@MnO_x can effectively generate H^+ in a weakly acidic environment, which promotes the degradation of MnO_x and further release of GOx.	[122]
COF_{FePc}		As pH decreases COF_{FePc} NSs target lysosomal aggregates, allowing them to exhibit excellent multi-enzyme mimicry including GSHOx in acidic lysosomes.	[87]
PEG/Ce-Bi@DMSN	Temperature responsiveness	High temperature enhances the activity of PEG/Ce-Bi@DMSN to mimic GSHOx, thereby promoting its consumption of GSH.	[20]
PEG- chitosan/PDA		The ability to deplete GSH increases with increasing temperature.	[92]
$Cu_2O@Mn_3Cu_3O_8$		After 1064 nm laser irradiation, the intracellular GSH content of CT26 cells decreased from 70% to 30%.	[89]
PDA-CD/POM@GOx/HA		Accelerated GSH depletion by photothermal effects induced by 808 nm laser irradiation	[142]
AuPt@Cu-PDA		After NIR irradiation, the intracellular Cu^{2+} content was significantly enhanced, and the excess Cu^{2+} acted as an oxidant to deplete intracellular GSH.	[143]
PEG-Cu_2WS_4	GSH responsiveness	In the TME, CWP NPs catalysed GSH oxidation close to or already at Vmax.	[88]
Cu-O_2/Cu-O_4 Sazyme		DMON depletes a portion of GSH in the tumour cells, synergising with Cu SAzyme to achieve a dual depletion of GSH.	[97]
COF_{FePc}		High concentrations of GSH increased the dispersion of COF_{FePc} NSs due to their responsiveness to GSH.	[87]
$CuMnO@Fe_3O_4$		The R1 and R2 relaxation rates of the $CuMnO@Fe_3O_4$ NPs demonstrated a positive correlation with the increase in GSH and H^+ concentrations, thereby validating the T1 and T2 contrast enhancement resulting from GSH and H^+ activation.	[144]

(*Continued*)

Table 4 (Continued).

Depleting GSH Nanozymes Formulation	Responsiveness	Feature	References
T-BTO/MoS_2		As the concentration of H_2O_2 increased, the absorbance at 652 nm also increased significantly.	[128]
Cu-Pd@MIL-101		The nanozyme mimics SOD and replenishes H_2O_2 levels in cells.	[145]
PtMnIr			[133]
Co/La-PB@MOF-199/GOx	H_2O_2	The pH response of MOF-199 allows accurate release of GOx into tumours to catalyse the reaction of glucose and O2 to produce H_2O_2.	[91]
Ce–Gd@CDs–GOx	responsiveness	The absorbance at 405 nm of Ce-Gd@CDs-GOx introduced with GOx was significantly higher than that of NPs not containing GOx	[146]
Cu_{2-x}Se-GOx		Cu_{2-x}Se-GOx exhibited enhanced green fluorescence, further substantiating that GOx-mediated H_2O_2 production augmented the analogue POD activity of Cu_{2-x}Se-GOx.	[94]
PtMnIr	Local electrical stimulus responsiveness	The local electrical current stimulus enhanced the activity of PtMnIr to mimic GPx, which led to the depletion of GSH.The XPS results suggested that this was due to the fact that the current stimulus altered the oxidation state of the metal and led to the release of the metal ions into the surrounding environment.	[133]
T-BTO/MoS_2	US responsiveness	BTO/MoS_2 induced significant GSH depletion mediated by US and caused up to 76.3% GSH loss after 6 h.	[128]
Fe^{2+}-Janus nanocomplexes		US increases production of -O^{-}_2.	[93]
Mo-doped Cu_9S_5		During US excitation, the yield of NO gas produced by m-MCS@LA was increased.	[147]

PH Responsiveness

Increased acidity is a feature of hypoxic tumors and their TME.[148] In general, normal cells only produce lactate during hypoxia and obtain energy through aerobic respiration and lactic acid fermentation. In tumor cells, downstream glycolytic enzymes are over-expressed to meet the energy demands caused by rapid tumor cell division. In malignant tumors, an extracellular pH of 6.5–6.9 (physiological pH 7.2–7.4) is typically observed, due to the high anaerobic metabolism of the tumor tissue, which results in the production of large amounts of acid.[149–151] Under acidic conditions, the spatial structure of natural enzymes is altered, rendering them inactive. In contrast, the nanozymes exhibited superior anti-tumor properties in acidic TME, greatly expanding their application as anti-tumor drugs.

Liu et al[102] designed Au-Cu^{2+}-ZIF-DOX (ACD) nanozymes with pH-responsive drug release and the ability to consume GSH, which reduces drug leakage in normal tissues and achieves rapid release in acidic TME. When ACD was subjected to pH 7.4, the drug was released at a slow rate, with a cumulative release of 5.82% after 36 h. Upon reduction of the pH to 5, degradation of ZIF-8 under acidic conditions led to an increase in the release of the drug, with a cumulative release of up to 41.97% after 36 h. Chen et al[128] synthesised thin layers of MoS_2 NSs on the surface of piezoelectric tetragonal barium titanate (T-BTO). After pH-responsive cinnamaldehyde (CA) modification, acidic TME-responsive nanocatalysts (T-BTO /MoS_2@CA) were prepared with the ability to mimic POD and GSHOx. T-BTO/MoS_2 exhibited good stability in an acidic environment (pH 1.6–6.0), and the pH-responsive CA release-mediated H_2O_2 self-supply provided sufficient substrate for its POD mimicry. A limitation of this study is that the ability of the nanoenzymes to consume GSH under different pH conditions was not separately investigated. Bai et al[121] proceeded to prepare HA-$CuMnO_x$ nanocomposites and investigate the effect of pH on GSH consumption. The absorbance values of DTNB at 405 nm were 0.659, 1.344, 1.352, 2.045, and 2.057 when the pH

was equal to 3, 5, 6, 7, and 8, respectively. These values indicate that the acidic condition enhanced the activity of the nanomaterials to mimic GSHOx and was more favourable for GSH consumption. In order to gain further insight into the underlying mechanism, the impact of pH on the release of Mn ions was investigated. The results demonstrated that approximately 40% of Mn ions were released from HA-CuMnO_x when pH = 7.4 and GSH was present, with this percentage increasing to 62% with increasing acidity. This indicates that the accelerated GSH depletion under acidic conditions may be associated with the increased release of Mn^{4+}. Furthermore, the release of Mn, Fe and Cu ions from the CuMnO@Fe_3O_4 core-shell nanozyme designed by Zhang et al[144] has also been demonstrated to be pH-dependent. Recently, Yan et al[152] developed acid-responsive, iron-coordinated polymer nanoparticles (PPA/TF) encapsulating the mitochondria-targeting drug α-tocopheryl succinate (α-TOS). In the weakly acidic intracellular environment of tumors, PPA/TF further promoted pH-responsive drug release and caused ferroptosis.

The pH-dependence exhibited by the aforementioned nanozymes indicates that lowering the pH of the TME will provide a more optimal environment for the nanozymes to deplete GSH against tumors. Hao et al[122] prepared a bismuth-manganese core-shell nanoflower containing glucose oxidase (GOx), designated BDS (Bi-DOPA@BSA)-GOx@MnO_x, with the capacity to deplete GSH. GOx catalysed the production of glucose from glucose, acidifying the TME. Experimental results demonstrated that there was no significant change in the pH of the BDS@MnO_x solution under either acidic (pH=6.5) or neutral (pH=7.4) conditions. In contrast, the pH of the simulated TME solution with the addition of BDS-GOx@MnO_x changed significantly, decreasing by approximately 3.4 in 8 h, whereas it only decreased by 1.0 under neutral conditions. This suggests that GOx plays an important role in regulating pH, and that BDS-GOx@MnO_x can efficiently generate H+ under weakly acidic environments, thus promoting the degradation of MnO_x and the further release of GOx. Furthermore, lysosomes, acidic organelles with a pH range of 3.5 to 5.5, are highly prevalent in tumor cells.[153,154] The development of nanozymes capable of lysosomal aggregation is also anticipated to enhance their ability to consume GSH. Lu et al.[87] A novel acid-responsive self-assembly strategy based on FePc-rich COF NSs was developed, which enabled the lysosome-targeting of COF_{FePc} NSs due to their abundant negative hydroxyl groups and rigid structure. TEM and atomic force microscope images demonstrated that COF_{FePc}NSs exhibited uniformly thick nanosheets at pH=4, in comparison to the morphology of COF_{FePc}NSs at pH 7, which suggests that COF_{FePc}NSs can self-assemble in acidic solution. Dynamic light scattering was used to measure the size of the nanomaterials in solution. The results showed that the hydrodynamic diameter increased with decreasing pH, indicating that the COF_{FePc}NSs gradually underwent aggregation. In particular, the hydrodynamic diameter increased significantly within a short period of time at pH 4. COF_{FePc} NSs target lysosomal aggregates, allowing them to exhibit excellent multi-enzyme mimicry including GSHOx in acidic lysosomes. This provides a promising opportunity to combine with other therapeutic strategies, such as PDT, CDT, and SDT, to enhance anti-tumor effects.

Temperature Responsiveness

The development and growth of tumors is closely linked to the local temperature of the tumor cells. Numerous studies have reported that when the local temperature of the tumor rapidly rises above 42°C, it causes cell rupture or denaturation of proteins to kill the tumor cells.[155–157] Previous studies have often considered tumor temperature regulation from a macroscopic perspective and rarely from a TME perspective.[158,159] However, in the case of GSH-consuming NPs enriched in tumor tissue, the site where they generate heat in the presence of NIR is in the TME. It is also in the TME that the nanozymes showed stronger enzymatic activity with increasing temperature within a certain range. Therefore, we categorise temperature as an element of the TME and investigate the responsiveness of GSH-consuming nanozymes to temperature.

Lin et al[20] developed a multifunctional bacteriophage-like PEG/Ce-Bi@DMSN nanozyme by decorating ultra-small CeO_2 nanozymes on large mesopores of Bi_2S_3@DMSN. The profile of the PEG/Ce-Bi@DMSN nanozyme in the presence of 25 °C and 50 °C on GSH depletion was investigated separately. The PEG/Ce-Bi@DMSN nanozymes exhibited a reduction in absorbance at 412 nm at 50 °C relative to 25 °C at 5, 10, 15 and 20 min of reaction. It was shown that high temperature enhanced the activity of PEG/Ce-Bi@DMSN mimicking GSHOx, thus promoting its consumption of GSH. Chiang et al[92] prepared and measured the GSH consumption ability of PEG-chitosan/PDA at 25 °C, 37 °C and 50 °C, respectively. The results showed that the GSH consumption capacity of PEG-chitosan/PDA increased with increasing temperature. Hou et al[89] prepared Cu_2O@$Mn_3Cu_3O_8$ (CMCO) and co-incubated it with CT26 cells to decrease the intracellular GSH content to approximately 70%. Following 1064 nm laser irradiation, the intracellular GSH content decreased to 30%. Cheng et al[142]

constructed a nanocomposite, PDA-CD/POM@GOx/HA (PCPGH), containing polymetallic oxyacid (POM) using β-cyclodextrin (β-CD) functionalised polydopamine (PDA-CD) as a matrix. Following irradiation with an 808 nm laser for a duration of six minutes, the temperature of the 50 μg/mL PCPGH solution reached 60 °C. In comparison to the PCPGH group, there was a notable increase in GSH consumption following laser irradiation. This suggests that the photothermal effect induced by 808 nm laser irradiation accelerates the process of GSH consumption. Liu et al[143] prepared Cu-PDA and AuPt@Cu-PDA nanoplatforms, respectively. In 4T1 cells, both Cu-PDA+NIR and AuPt@Cu-PDA+NIR depleted GSH more than Cu-PDA and AuPt@Cu-PDA alone (Figure 5). In order to further investigate the mechanism of accelerating GSH by photothermal effect, the intracellular Cu^{2+} content was measured. It was observed that following NIR irradiation, the intracellular Cu^{2+} content was markedly elevated, with the surplus Cu^{2+} acting as an oxidant to deplete the intracellular GSH. This indicates that the heightened temperature responsiveness of such nanozymes' capacity to deplete GSH may be associated with their excess of heavy metal ions with oxidative capacity released at elevated temperatures. In comparison to natural enzymes, nanozymes exhibit a broader temperature range within which they are able to exert their activity. It is also encouraging to note that the catalytic effect of the nanozyme can be enhanced by increasing the temperature within a certain range. This provides a solid foundation for glutathione-depleted nanozymes in photothermal therapy (PTT) and PDT applications.

Substrate Responsiveness

High levels of GSH (≈10×10^{-3} M) and H_2O_2 ($50 \sim 100 \times 10^{-6}$ M) in tumor cells provide substrates for GSH-depleting nanozymes.[160,161] It is and its essential to probe the responsiveness of the nanozymes to GSH and H_2O_2 in an environment that mimics TME.

Glutathione Responsiveness

As mimics of natural enzymes, GSH-depleted nanozymes also exhibit the general pattern of enzymatic reactions in terms of the rate of initiation in relation to substrate concentration. Hao et al[88] investigated the enzymatic reaction rates of CWP NPs corresponding to different GSH concentrations (0–3 mm) and fitted the Michaelis-Menten equation. As the GSH concentration approached 3 mm, the rate at which the CWP NPs mimicked the GSHOx enzymatic reaction had stabilized. It can be surmised that the GSH oxidation catalyzed by CWP NPs under the stimulation of GSH in the tumor microenvironment is approaching or has reached its V_{max}. Lin et al[97] devised a strategy for the in-situ synthesis of Cu SAzyme, whereby the GSH-responsive deformability of DMON is employed to convert adsorbed copper ions into isolated atoms anchored by oxygen atoms ($Cu\text{-}O_2$/$Cu\text{-}O_4$). During this process, DMON also consumes a portion of GSH

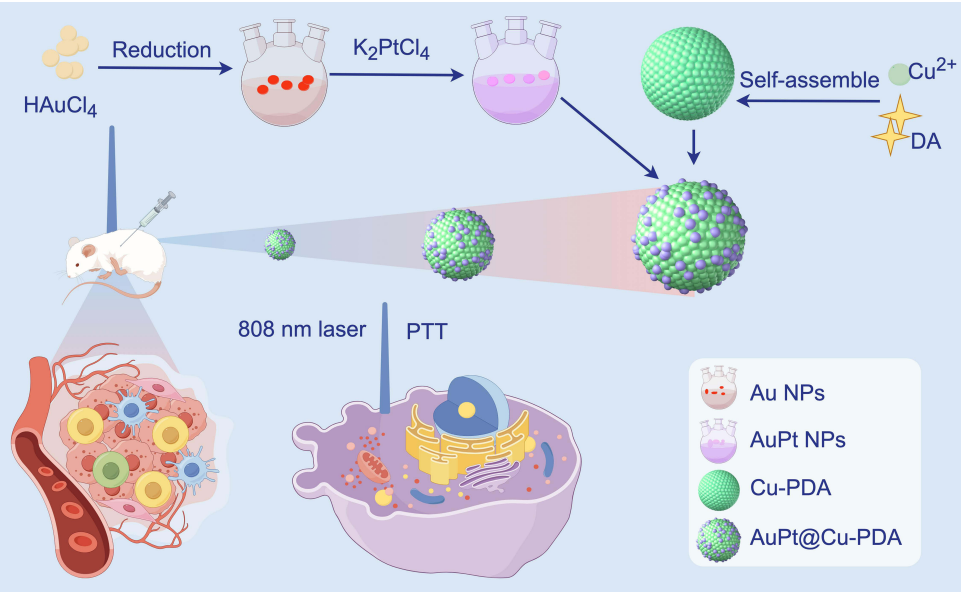

Figure 5 AuPt@Cu-PDA NPs with photothermal conversion effect were synthesized by Liu et al (By Figdraw).

within tumor cells, resulting in the dual depletion of GSH. Lu et al[87] proceeded to prepare COF_{FePc} NSs and test their stability following incubation with varying concentrations of GSH. These concentrations were 10×10^{-3}, 1×10^{-3} and 0.1×10^{-3} M. The results demonstrated that the size of COF_{FePc} NSs exhibited a significant increase in the COF_{FePc} NSs +1 and 10×10^{-3} M GSH groups. Nevertheless, the dimensions of the COF_{FePc} NSs+0.1×10^{-3}M GSH group remained largely unaltered. High concentrations of GSH increased the dispersion of COF_{FePc} NSs due to their responsiveness to GSH. Following the application of 1 mm GSH, some of the building blocks were observed to separate from the FPIC NPs prepared by Ye et al,[104] resulting in a slight decrease in particle size. Upon increasing the GSH concentration to 5 mm, the nanostructures exhibited a complete collapse, resulting in optimal dispersion, which is consistent with the data analyzed by dynamic light scattering. The reason for this phenomenon may be since Pt ions have a stronger affinity for S oligopeptides than they do for O atoms. Furthermore, drug release profiling demonstrated that up to 62% of curcumin was released from FPIC NPs following incubation with GSH (5 mm) for 24 h, which was considerably higher than the release of curcumin in the absence of GSH. The GSH-responsive FPIC nanoparticles exhibited good dispersion and physiological stability in the TME, which facilitated the achievement of site-specific drug release and the minimization of in vivo toxicity. Furthermore, the GSH response facilitates tumor imaging. Zhang et al[144] demonstrated that their prepared CMF NPs exhibited both imaging and GSH-consuming properties. The R1 and R2 relaxation rates of the CMF NPs demonstrated a positive correlation with the increase in GSH and H^+ concentrations, thereby validating the T1 and T2 contrast enhancement resulting from GSH and H^+ activation. The same changes were also observed in the MRI results. Consequently, the dual activation of T1 and T2 signals and the depletion of GSH provide a robust foundation for the activation of CDT and MR signals in TME.

H_2O_2 Responsiveness

A number of GSH-depleting nanozymes also possess the capacity to mimic the activities of POD and CAT. POD-mimicking nanozymes convert endogenous H_2O_2 to H_2O and ROS, while CAT-mimicking nanozymes convert endogenous hydrogen peroxide H_2O_2 to oxygen O_2.[162–164] This approach is particularly attractive in hypoxic TME. The high concentration of H_2O_2 in tumor cells provides a sufficient substrate for GSH-depleted nanozymes that mimic the catalysis of POD and CAT. The T-BTO/MoS_2 nanozymes prepared by Chen et al[128] demonstrated the capacity to mimic POD while consuming GSH. The -OH generated by the POD oxidizes the colorless 3.3',5,5'-tetramethylbenzidine (TMB) to blue oxidized TMB. Following the reaction of T-BTO/MoS_2 with different concentrations of H_2O_2 (0.2, 0.4, 0.6, 0.8, 1 mm), the absorbance at 652 nm was detected. The results demonstrated a significant increase in absorbance at 652 nm in response to an increase in H_2O_2 concentration. Furthermore, the aforementioned gap exhibited a gradual increase over time, spanning from 0 to 10 min. Lin et al[93] prepared a biocatalytic Janus nanocomplex (termed UPFB) containing Fe^{2+} to mimic GSHOx. During this process, Fe^{2+} catalyzed the formation of -OH from endogenous H_2O_2 via the Fenton reaction. The absorbance at 652 nm was examined for the reaction of UPFB with different concentrations of H_2O_2 (5, 10, 25, 50, 100 uM). The results demonstrated that the absorbance at 652 nm increased significantly with the increase of H_2O_2 concentration.

There is evidence that POD and CAT enzymatic reactions occur, and that there may be a deprivation of H_2O_2 in tumor cells.[165] Replenishment of H_2O_2 is highly correlated with the efficiency of CDT, PDT, and other similar processes.[166,167] Therefore, it is also necessary to consider the H_2O_2 replenishment ability of nanozymes when designing them. About the supplementation of H_2O_2 by nanozymes, two principal approaches may be identified. One approach is to equip the nanozymes with the capacity to mimic SOD, enabling them to catalyze the disproportionation of $-O^-_2$ to generate O_2 and H_2O_2. Li et al[145] modified 9.5 wt%Cu-Pd@MIL-101 (9.5% CPMP) with a PEG-modified, which is a nanozyme with simultaneous POD, SOD and glutathione depletion. The highly water-soluble tetrazolium salt (WST) can react with $-O^-_2$ to form a water-soluble dye with a strong UV-vis absorption signal at 440 nm. The ability of different concentrations of 9.5% CPMP to mimic SOD was evaluated using this method, and it was found that the absorbance at 440 nm gradually became smaller as the concentration of 9.5% CPMP increased. The PtMnIr NPs designed by Hu et al[133] also possessed SOD activity, and the absorbance of the solution decreased with increasing concentration of PtMnIr NPs. This evidence indicates that NPs deplete $-O^-_2$ by mimicking SOD and replenish the level of H_2O_2 in tumor cells. A second method of supplementing H_2O_2 is to modify the nanomaterials with GOx. GOx catalyses the reaction between glucose and oxygen to form gluconic acid and H_2O_2.[168,169] Wang et al[91] prepared Co/La-PB@MOF-199/GOx for the self-supply of H_2O_2 in

TME by loading GOx onto Co/La-PB@MOF-199. The particle size of Co/LaPB@MOF-199/GOx was significantly reduced at pH 5.8, as demonstrated by dynamic light scattering assay. This is due to the pH-responsive nature of MOF-199, which results in a certain degree of nanoparticle decomposition in the TME. This enables the precise release of GOx into the tumor, where it catalyzes the reaction of glucose and O_2 to produce H_2O_2. Ce-Gd@CDs-GOx nanozymes were prepared by Sun et al.[146] The probe used to detect H_2O_2 generation was titanium oxide sulfate (Ti $_{(IV)}$ OSO_4). Upon oxidation by H_2O_2, Ti $_{(IV)}$ OSO_4 forms a yellow perovskite complex, Ti $_{(IV)}$ O_2SO_4, with characteristic UV absorption at 405 nm. The absorbance at 405 nm of Ce-Gd@CDs-GOx nanozymes with GOx incorporated was significantly higher than that of NPs without GOx, indicating that the prepared nanozymes were capable of producing more H_2O_2 through the catalytic reaction of GOx. Ye et al[94] designed $Cu_{2-x}Se$-GOx NPs and evaluated the intracellular -OH content in the presence of $Cu_{2-x}Se$ and $Cu_{2-x}Se$-GOx using the 2.7-dichlorodihydro-fluorescein diacetate as an indicator. Notably, $Cu_{2-x}Se$-GOx exhibited enhanced green fluorescence, further substantiating that GOx-mediated H_2O_2 production augmented the analogue POD activity of $Cu_{2-x}Se$-GOx. Similarly, the supply of H_2O_2 by GOx was confirmed in the nanozymes prepared by Lin[170] and Cheng et al.[142]

Other Factor

The GSH-depleted nanozymes were also responsive to local electrical current stimulation and US. Hu et al[133] employed the sulfhydryl tracer violet method to detect the GSH depletion process in vitro. The PtMnIr+E group exhibited a reduction in green fluorescence compared to the PtMnIr and E groups following electrical treatment. This suggests that local electrical current stimulus enhances the activity of PtMnIr to mimic GPx, thereby depleting GSH. To ascertain the mechanism by which electrical treatment enhances PtMnIr enzyme activity, XPS results were further compared between PtMnIr and PtMnIr+E. It was observed that the concentrations of Pt^{2+}, Mn^{3+} and Ir^{3+} increased significantly, from 18.9%, 35.7% and 20.2% to 31.5%, 46.3% and 40.6%, respectively. It can be concluded that the observed increase in GPx activity is a consequence of the current stimulation, which alters the metal oxidation state and results in the release of metal ions into the surrounding environment. The T-BTO with piezoelectric properties, designed by Chen et al,[128] demonstrated enhanced enzymatic activity of GSHOx when subjected to US-mediated charge generation. In comparison to the control and BTO/MoS_2, BTO/MoS_2 induced a significant depletion of GSH under US-mediated conditions, resulting in a loss of up to 76.3% GSH after 6 h. Under US irradiation, BTO undergoes mechanical deformation and generates induced surface charges promoting the consumption of GSH by BTO/MoS_2. The UPFB NPS were prepared by Lin et al[93] and were used to confirm the ability to produce -O^-_2 by singlet oxygen generation efficiency (ΦΔ). The ΦΔUPFB value for 808 nm laser and US irradiation without H_2O_2 addition ($\Phi_{\Delta UPFB}$ = 0.016) was significantly larger than that for 808 nm laser irradiation only ($\Phi_{\Delta UPFB}$ = 0.012). Furthermore, Hou et al[147] constructed a nanozyme, m-MCS@LA, which is a loaded L-arginine mesoporous Mo-doped Cu_9S_5 nanozyme. The yield of NO gas produced by m-MCS@LA was increased during US excitation. Yang et al[75] also demonstrated that after 5 min of ultrasound stimulation, N-acetyl-L-cysteine released approximately 19.57 μm of NO, which was significantly higher than the release of NO in the N-acetyl-L-cysteine group alone. NO gas molecules not only exerted a synergistic effect through gas therapy but also enhanced the effect of CDT by inhibiting protective autophagy.

In the preceding four subsections, we have separately discussed the response of GSH-depleted nanozymes to different factors. In the design of actual nanozymes, however, these factors are not split. For instance, nanozymes that modify GOx are responsive to both pH and H_2O_2. It is a common practice among scholars to design nanozymes with multi-factor responsive properties with the intention of achieving more effective anti-tumor effects. Furthermore, the responsiveness of nanozymes to different factors has led to the development of various tumor therapies, including nanozymes-based CDT, PDT, SDT, and so forth.

Nanozymes Depleting Glutathione in Oxygen-Dependent Cancer Therapy

Nanomaterial-mediated ODCT (eg, CDT, PDT, SDT) has attracted considerable attention from scholars due to its remarkable efficacy.[171–173] GSH-depleted nanozymes induced a ROS ‘explosion’ in TME through a cascade reaction between GSHOx, GPx, CAT, OXD, POD, and SOD. This section will present a systematic introduction to the innovative

concept of combining GSH-depleting nanozymes with key anti-cancer pathways to construct bio-inspired synergistic cancer therapies based on the ODCT perspective.

Chemodynamic Therapy

CDT represents a novel class of tumor therapeutic technology that exploits the TME to trigger the Fenton (Fenton-like) reaction of nanomedicines, thereby producing potent oxidative radicals, such as -OH, for tumor-specific treatment. In comparison with conventional therapies, CDT exhibits enhanced tumor specificity, selectivity, reduced systemic toxicity and a diminished risk of side effects.[174,175] Nevertheless, However, the use of CDT is severely hampered by GSH for -OH scavenging and insufficient levels of H_2O_2 within malignant tumors. The construction of CDT nanosystems with high yield and full utilization of ROS at the tumor site represents a significant area of research within the field of CDT. This subsection describes six GSH-consuming nanozymes for CDT.

Liu et al[102] synthesised Au NCs and DOX loaded, copper ion-doped ZIF-8 nanoplatforms (ACDs) for the purpose of TME-activated tumor CDT and combination chemotherapy. Upon the gradual degradation of Cu^{2+}-doped ZIF-8 in an acidic TME, Cu^{2+}, DOX, and Au NCs were released. The Cu^{2+} ions consumed GSH via redox reactions, and the generated Cu^{+} mimicked POD to convert internal H_2O_2 to -OH. In addition, the Au NCs not only consumed GSH as GSHOx, but also mimicked POD to catalyze the conversion of H_2O_2 to -OH. The enhanced tumor CDT was achieved by GSH depletion, elevated H_2O_2 levels and sufficient -OH. In addition, the chemotherapeutic effects were enhanced by the inhibition of DOX efflux and increased drug sensitivity due to GSH depletion and -OH generation. Hao et al[122] prepared TME-responsive BDS-GOx@MnO_x, which enhanced CDT by depleting GSH and glucose as well as generating a high concentration of -OH. In particular, MnO_x nanoflowers formed on Bi exhibited the capacity to respond to acidic TME, depleting GSH and releasing GOx, which initiated a glycolytic reaction. This resulted in a reduction in intracellular acidity in tumor cells and the generation of substantial quantities of H_2O_2, which ultimately led to an enhanced Fenton reaction. The multi-enzyme cascade of starvation therapy and CDT, in conjunction with the aforementioned processes, resulted in BDS-GOx@MnO_xNPs exhibiting excellent anti-tumor capabilities both in vivo and ex vivo. Furthermore, BDS@MnO_x enhanced CT and MR imaging, thereby facilitating the diagnosis and treatment of malignant tumors. Sun et al[21] designed DMSN-Au-Fe_3O_4 NPs grafted with a GLS inhibitor (CB839). These nanozymes, which block the glutamine pathway and GSH biosynthesis, and decrease ROS depletion at the tumor site, are catalytically converted to H_2O_2 by GOx-mimicking AuNPs. Subsequently, the compound was converted to -OH by POD-mimicking iron oxide nanoparticles. The combined action of the three components resulted in a significant increase in intracellular ROS levels and a notable enhancement in the efficacy of the CDT process. The 9.5% CPMP prepared by Li et al[145] demonstrated the capacity to mimic POD, SOD and GSHOx. The 9.5% CPMP was found to mimic SOD, thereby compensating for the lack of H_2O_2 in tumor cells. The combination of POD and GSHOx was observed to elevate the level of -OH and maintain high oxidative stress in tumor cells. The results of in vivo experiments demonstrated that the stable 9.5% CPMP NPs exhibited effective CDT effects on tumors, with good biosafety and biocompatibility. Ye et al[94] designed Cu_{2-x}Se-GOx for TME-triggered cascade catalysis, with the objective of enhancing cancer therapy. Among the components of this system, Cu_{2-x}Se has the capacity to mimic GSHOx effectively oxidizing GSH, thereby reducing the consumption of ROS. Additionally, Cu_{2-x}Se serves as a mimic of CAT, catalysing the conversion of H_2O_2 to O_2 in cancer cells. Subsequent to this, GOx consumes a significant quantity of intracellular glucose, with the assistance of O_2. This process not only elevated the acidity of the tumor cells but also generated highly cytotoxic -OH due to the POD activity of Cu_{2-x}Se. Cui and colleagues[146] were successful in the construction of a Ce-Gd@CDs-GOx nanozyme platform. The nanozymes demonstrated high catalytic efficacy in promoting -OH generation and glucose oxidation, thereby achieving synergistic anticancer activities of nanocatalysis and starvation therapy. Furthermore, due to Gd^{3+} doping, these nanozymes can be used for T1-weighted MRI to guide precise treatment.

Photothermal Therapy and Photodynamic Therapy

The use of PTT in the treatment of tumors was inspired by magnetothermal therapy and was first reported by Hirsch et al[176] in 2003. Upon exposure to NIR, the photosensitive NPs convert the absorbed light energy into thermal energy, resulting in a rapid increase in local temperature above 42°C, which effectively kills tumor cells.[177] Concurrently, these nanoparticles will transfer the energy to the surrounding oxygen, thereby generating highly active singlet oxygen.

Monomorphic oxygen can react with nearby biomolecules in an oxidative manner to generate ROS, thus enabling PDT of tumors.[178,179] This subsection describes 10 GSH-consuming nanozymes for PTT and PDT.

The PEG/Ce-Bi@DMSN nanozymes prepared by Lin et al[20] exhibited CAT mimetic activity and GSH depletion capacity. This weakened the antioxidant defences of tumor cells and made the cells more sensitive to ROS. Among these, CeO_2 nanozymes catalyzed the Fenton-like reaction to produce highly toxic -OH in acidic TME. The activation of PTT by Bi_2S_3 in the NIR-II region significantly enhanced POD-mimic, CAT-mimic activities and GSH depletion. The HA-$CuMnO_x$@ICG nanozymes constructed by Bai et al[121] not only have CAT, and GSH consuming ability. It also mimics that POD can convert intracellular H_2O_2 into highly toxic ROS. HA-$CuMnO_x$@ICG-mediated PTT facilitates the catalytic reaction of the nanozymes and promotes the generation of ROS. Zhu et al[132] synthesised $CoSnO_3$, which exhibited triple enzyme-like catalytic activity. This included CO^{2+}-mediated POD-like catalysis for ROS production, Sn^{4+}-mediated depletion of overexpressed GSH, and also achieved catalytic decomposition of endogenous H_2O_2. The photothermal conversion efficiency of $CoSnO_3$ NPs was as high as 82.1% at 1064 nm NIR. With NIR, the triple enzyme-like catalytic activity of $CoSnO_3$ NPs was further enhanced to facilitate the development of a fully integrated multimodal tumor therapy. The Fe^{3+}@PEG-CS/PDA nanozymes, designed by Chiang et al,[92] exhibited remarkable photothermal conversion efficiency and structural stability, in addition to acid-triggered Fe^{3+} release. The Fe^{3+} chelating nanozymes converted H2O2· to OH via GSH depletion and heat/acid enhancement of the Fe^{2+}/Fe^{3+}-mediated Fenton's catalytic reaction. The PDA-mediated Michael reaction and Fe^{3+}/Fe^{2+} redox coupling resulted in a substantial depletion of intracellular GSH. It was demonstrated that Fe^{3+}@PEG-CS/PDA nanozymes were effective in increasing intracellular GSH depletion and -OH production in NIR-triggered thermotherapy. Wang et al[91] synthesised Co/La-PB@MOF-199/GOx, which could achieve self-supply of H_2O_2 by encapsulation of MOF-199 and loading of GOx. Meanwhile, due to the CAT and POD-like activities of Co/La-PB@MOF-199, the successive production of -OH was achieved by the multienzymatic cascade under NIR for photothermal enhanced catalytic therapy. Cheng et al[142] designed PDA-CD/POM@GOx/HA, in which GOx catalyzes the conversion of glucose to H_2O_2 and gluconic acid. POM mediates the generation of -OH, depleting the intracellular GSH pool. PDA-POM-mediated photothermal enhancement of the multi-enzyme cascade catalytic and GSH depletion activity ultimately triggers apoptosis-ferroptosis, which is a form of synergistic tumor therapy. Zhang et al[144] prepared PCMF nanoplatforms by binding a platelet-derived growth factor receptor-β-recognising cyclic peptide target to the surface of CMF. In the presence of TME conditions, PCMF decomposed and produced a number of Fenton-catalytic active metal ions (eg, Cu^{+}, Mn^{2+}, and Fe^{2+}) with Fenton catalytic activity. This process resulted in a significant depletion of GSH, the acceleration of Fenton and Fenton-like reactions, the elevation of ROS levels, and the induction of apoptosis and ferroptosis in cancer cells. Furthermore, PCMF demonstrated the capacity to activate the T1 relaxation rate (23.15 $mM^{-1}s^{-1}$) and T2 relaxation rate (177.5 $mM^{-1}s^{-1}$), which facilitated tumor imaging. The COF_{FePc} developed by Lu et al[87] demonstrated satisfactory photothermal performance under NIR. In acidic conditions, COF_{FePc} exhibited good OXD-, SOD- andPOD-like activities and efficiently produced more -OH through a self-cascade reaction. The synergistic effect of toxic -OH and photothermal energy enabled COF_{FePc} NSs to accumulate in lysosomes, leading to lysosomal membrane permeability and apoptosis. The release of COF_{FePc} NSs from damaged lysosomes allows for further consumption of GSH and the production of H_2O_2. This amplifies oxidative stress through significant GSHOx-like activity, inducing ferroptosis in tumor cells. The POD and CAT-like activities of AuPt@Cu-PDA, prepared by Liu et al,[143] facilitate the generation of -OH and O_2 from H_2O_2. O_2 can be further converted to toxic $-O^{-}_2$ by its OXD mimetic activity. This effect is further enhanced by the remarkable photothermal properties of AuPt@Cu-PDA. In addition, Cu^{2+} can effectively deplete endogenous overexpressed GSH, thereby amplifying oxidative stress. Most importantly, excessive accumulation of Cu^{2+} disrupts copper homeostasis, leading to aggregation of lipoylated dihydrolipoamide S-acetyltransferase and ultimately cuproptosis. In a simulated TME, the core-shell structured CMCO nanozymes synthesized by Hou et al[89] were found to induce high efficiency ferroptosis-boosted-cuproptosis through mild photothermal effects. Due to the Cu^{+}/Cu^{2+} and $Mn^{2+}/Mn^{3+}/Mn^{4+}$ redox pairs, CMCO nanoenzymes exhibit a variety of enzyme-mimicking activities, including GSHOx-like, POD-like, and CAT-like activities. CMCO mimics GSHOx to consume GSH, which reduces the ability to chelate copper ions, exerts copper toxicity, and induces cuproptosis in cancer cells. The CAT-like activity catalyzes the generation of O_2 from H_2O_2, which enhances cuproptosis. Moreover, based on the Fenton - like reaction, and iron death caused by GSH elimination induced by GPX4 inactivation. This is accompanied by the lipid peroxidation (LPO) and the accumulation of ROS, which cleave stress-induced heat shock proteins, thereby reducing their protective capacity against cancer cells and further sensitising cuproptosis. Zhang et al[180] designed a tumor

cell-targeted nanomimetic delivery system that improves hypoxia, responds to TME, and efficiently loads ICG. Providing a new strategy for cost-effective and convenient synergistic treatment of cervical cancer with PTT and CDT.

Sonodynamic Therapy

SDT represents a novel, non-invasive and precise method of tumor treatment, in which NPs are employed as an efficacious acoustic sensitizer to "target" tumor cells and tumor neovascular endothelial cells in high concentrations.[181,182] Upon stimulation by ultrasound in vitro, NPs generate single oxygen species that cause tumor cell death.[183] This section describes two GSH-depleting nanozymes for SDT. Lin et al[93] prepared a biocatalytic Janus nanocomplex for both US-driven and 808 nm NIR light-mediated by combining core-shell-shell upconversion nanoparticles (UCNPs, NaYF4:20%Yb,1%Tm@NaYF4:10%Yb@NaNdF4) and iron-zirconium porphyrin metal-organic frameworks [PCN-224(Fe)] (called UPFB). It was shown that UPFB not only exhibited PDT performance under 808 nm laser irradiation, but also could be synchronously activated by US for SDT effect. Among them, Fe^{3+} mimicked CAT to catalyze the production of O_2 from H_2O_2 to alleviate hypoxia in TME, and it consumed excess intracellular GSH to promote ROS production. Meanwhile, in TME, Fe^{2+} converted by Fe^{3+} reacts with intracellular H_2O_2 to generate toxic -OH. In addition, UPFB can be used as a good contrast agent for fluorescence imaging and T2-weighted MRI, which provides precise guidance for tumor treatment. In a recent study, Yang et al[75] synthesized BCNR nanozymes (Figure 6). Under US sonosensitizers of Ce6 and RuO_2 exhibit highly efficient singlet oxygen. The SOD and CAT mimetic activities of RuO_2 further enhanced the sensitivity of Ce6 to ultrasound stimulation behavior. Concurrently, the cleavage of S-nitrosothiol group in BCNR liberated NO, which then reacted with singlet oxygen to spontaneously generate highly cytotoxic peroxynitrite (ONOO-). The antioxidant homeostasis in the TME was disrupted by the depletion of intracellular GSH due to the GPx mimetic activity of RuO_2 and the downregulation of the GR by ONOO-. Concurrently, the inhibition of GPX4 activity resulted in an enhanced iron death sensitivity of tumor cells. The efficacy of iron death was greatly enhanced with the accumulation of lipid hydroperoxide produced by ONOO-. In a recent study, Jiang et al[184] prepared small-sized iron-platinum nanoparticles using a thermal reduction method. The nanoparticles effectively decomposed H_2O_2 to generate O_2, reversing the tumor hypoxic environment. More satisfactorily, they generated

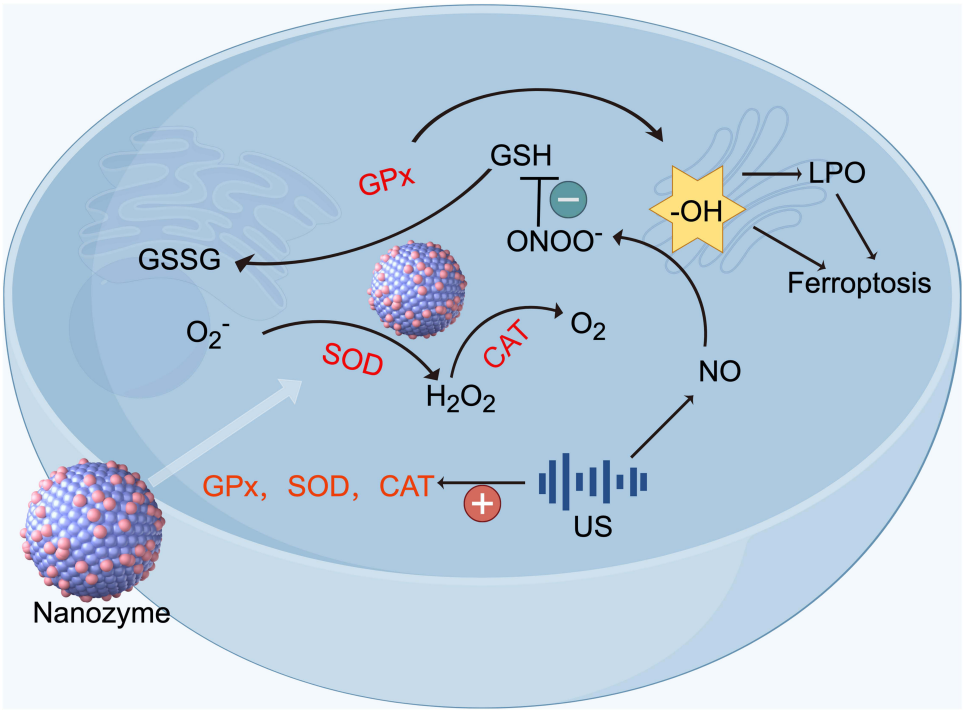

Figure 6 Under US, BCNR oxidized GSH and inhibited GR, ultimately leading to iron death. (By Figdraw).

https://doi.org/10.2147/IJN.S515734

single-linear state oxygen under ultrasound irradiation, thereby killing tumor cells and inhibiting their proliferation, which is potentially valuable in enhancing oxygen-enhanced sonodynamic cancer therapy.

In conclusion, in normal cells, oxidants represented by ROS and antioxidants represented by GSH are in a dynamic equilibrium, analogous to the yin and yang poles of the Chinese 'Tai Chi'. Nanozymes based CDT, PDT, SDT achieve an imbalance by increasing the anode (increasing ROS through GOx, POD, OXD) or decreasing the cathode (depleting GSH through GSHOx, GPx or inhibiting GSH production) to eliminate tumor cells.

Ferroptosis

Ferroptosis, a novel form of regulated cell death, is centrally characterized by the aberrant accumulation of iron-dependent lipid peroxidation and the inactivation of antioxidant defense systems. In recent years, NPs have emerged as a key tool in the regulation of ferroptosis due to their unique physicochemical properties.[152] Wang et al[116] created a bimetallic nanozymatic system (ZIF-8/SrSe) encapsulated with DOX. ZIF-8/SrSe nanozymes exhibit strong GSHOx-like activity and effectively oxidize reduced GSH to GSSG while inhibiting GPX4 and solute carrier family 7 member 11 (SLC7A11). This resulted in iron homeostasis imbalance, pronounced caspase activation, and subsequent induction of apoptosis and ferroptosis in tumor cells. The ChA CQDs designed by Zeng et al[110] exhibited significant GSHOx-like activity and subsequently promoted cancer cell ferroptosis by interfering with the lipid repair system catalyzed by GPX4.The DNA nanozymes designed and prepared by Zhou et al[185] inhibited hypoxia inducible factor-1α (HIF-1α) while achieving GSH depletion and cellular ferroptosis. Fe/Cu bimetallic nanozymes prepared by Wang et al[186] catalyzed the production of ROS and depletion of GSH from excess intracellular H_2O_2. Excess H_2O_2 and GSH are the major factors of radioresistance and chemoresistance, and their reduction enhances chemotherapy and radioisotope therapy. Produced ROS and depleted GSH further induce mitochondrial dysfunction. Promotion of lipoylated dihydrolipoamide S-acetyltransferase and aggregation of lipid peroxidation leads to ferroptosis and cuproptosis. In a recent study, Ir@Au nanozymes prepared by Lin et al[187] enhanced the radiosensitivity of tumors by disrupting the energetic homeostasis of tumor cells and inducing ferroptosis. It generated additional ROS for CDT, depleted GSH, and interfered with the tumor's antioxidant defenses. When exposed to ionizing radiation, the nanozymes absorb photons and emit electrons that interact with water to amplify ROS production. This ROS accumulation, in combination with radiation, enhances DNA damage and lipid peroxidation, reverses radiation resistance and promotes ferroptosis.

Target Treatment

Nanoparticle-based targeted therapy empowers nanocarriers with the ability to specifically recognize the site of a lesion through engineering for efficient drug enrichment and controlled release (Table 5). Xu et al[188] developed a platelet

Table 5 Nanozyme Targeting Therapy

Nanozymes	Strategies	Therapies	Features	References
Platelet membrane biomimetic monoatomic nanase	Platelet membrane modification	CDT, Immunological therapy	The double starvation effect significantly reduced the levels of intracellular glucose and ATP, resulting in a significant decrease in cellular GSH.	[188]
PdAg-CaP-L-buthionine sulfoximine	Hyaluronic acid surface modification	PTT	It is activated by near-infrared light, inducing photothermal and photodynamic effects, causing ROS bursts, and promoting apoptosis by triggering immunogenic cell death.	[189]
Cu-SAzymes	Bioorthogonal approach	PTT	The release of Cu ions in the presence of GSH induces cuproptosis.	[190]
CuMnO@Fe_3O_4	Coupled to platelet-derived growth factor receptors	PTT, CDT	The weak acid- and GSH-activated T1 and T2 relaxation rate of nanozyme contributes to T1 and T2 dual contrast imaging at the tumor site.	[144]
Aupd-GSH suppression system	Tumor homologous membrane camouflage	CDT, Chemotherapy	The nanozyme abrogates the reductive adaptation by exerting its molecule-targeted GSH suppression, thereby achieving a dual-disruption on cancer redox homeostasis.	[191]

membrane-mimicking single-atom nano-enzyme for cancer therapy. Due to platelet membrane modification, the nano-enzyme can effectively target tumors. Promoting ROS production in tumors enhanced the immune response, especially by increasing memory T cell abundance and inhibiting distant tumor growth and tumor metastasis. Jiang et al[189] developed a framework consisting of PdAg mesoporous nano-enzymes and CaP mineralised layers fitted with the GSH inhibitor L-buthionine sulfonamide. Further surface modification of hyaluronic acid allowed targeting of CD44. In acidic tumor microenvironments, Ca^{2+} is initially released, leading to mitochondrial dysfunction and ultimately apoptosis. Surprisingly, Fan et al[190] developed a new in situ bombarding-embedding technique for the ultra-fast synthesis of sputtered SAzymes. Sputtered copper SAzymes (CuSA) with unique planar Cu- C_3 coordination structures were prepared using this method. Bioorthogonal method was further employed to design CuSA with enhanced tumor-specific targeting. The nanoenzymes not only possessed minimal off-target toxicity, but also had ultra-high CAT, OXD, and POD polymerase activities to generate ROS storms for effective tumor destruction. Zhang et al[144] developed a TME-responsive CuMnO@Fe_3O_4 core-shell nanozymes, a platelet-derived growth factor receptor-β-recognising cyclic peptide target was coupled to the surface of the nanozymes to fabricate tumor-specific nanozymes with enhanced targeting capabilities, providing new insights into high-sensitivity and tumor-specific therapy. In a recent study, Bai et al[191] developed AuPd alloy nanozymes- GSH biosynthesis inhibitor co-donating nanozymes further camouflaged with tumor-homologous cell membranes to fabricate hybrid nano-systems with biostability and tumor-targeting capabilities, initiating safe and precise redox-destruction cancer-based therapies that and sensitizing standard chemotherapy.

Toxicity Reduction Strategy

How to reduce the toxicity of nanoparticles is an important research direction in the field of nanomedicine. Whether the application is anti-tumor, antibacterial or anti-inflammatory, biosafety is a prerequisite. Scholars often modulate the crystal phase of nanoparticles or use chemical or physical methods to modify and functionalize the surface of nanoparticles in order to enhance biocompatibility.[192,193] Wu et al[194] reported an amorphous ZIF-8 (aZIF-8) with a high loading of 5-Fu by pressure-induced amorphisation. aZIF-8 has a longer blood circulation and lower lung accumulation than ZIF-8 at the same injected dose, with less drug release and good biocompatibility, which significantly improves its therapeutic efficacy in ECA-109 loaded mice, with a survival rate of 50 days after treatment reaching 100%. Regarding the modification of nanoparticles, polyethylene glycol, polyvinylpyrrolidone can be used to encapsulate NPs, or to bind them to natural molecules such as albumin, which ultimately reduces the immune recognition by the immune system.[195–197] To avoid long-term toxicity of nanoparticles in the body, biodegradable materials can be preferred. Such as mesoporous silica and liposomes, which can reduce the toxicity and match its application cycle.[198–200] In addition, the metabolic tachycardia rate in vivo can be accelerated by designing the size and morphology of nanoparticles. Control particle size in the range of 5–100 nm to avoid capture by the mononuclear phagocytosis system.[201,202] Control the hydrated particle size to less than 5.5 nm to promote its excretion via urine and select spherical, lamellar or rod-like structures to regulate cellular uptake rates.[203–206] Moreover, pH response, temperature response, and substrate response can be utilised to control the reaction time, intensity, and release rate of the carried drug.[207–209] More promisingly, the enrichment characteristics of nanoparticles can be utilised to increase the enrichment of target tissues and reduce the exposure of non-target organs by means such as coupling antibodies or small molecule ligands.[210–212] In conclusion, the toxicity of nanomaterials can be reduced by surface modification and functionalisation, selection of biodegradable materials, design of size and morphology, stimulus responsiveness, and targeting. Among them, the targeting effect has far-reaching research value.

Summary and Prospect

Since the initial discovery of Fe_3O_4 NPs with POD-mimicking activity in 2007, nanozymes have emerged as a crucial area of research in the fields of medicine, healthcare and industry. In particular, nanozymes have demonstrated remarkable therapeutic efficacy in the field of oncology, inducing intracellular ROS ‘explosions’ in tumor cells via a multi-enzyme cascade of GSHOx, GPx, SOD, CAT, POD, and OXD. This paper presents an overview of the mechanism and role of GSH-depleting nanozymes in recent years, their classification, TME-responsiveness and application in ODCT. Although GSH-consuming nanozymes have made significant progress in the treatment of tumors, there are still some noteworthy challenges to be addressed.

(I) Selectivity: The issue of inadequate substrate selectivity in nanozymes remains unresolved, with the potential to impact therapeutic efficacy and even result in toxic side effects. Modifying the nanozymes to enable specific substrate recognition could enhance tumor targeting accuracy and sensitivity.

(II) Catalytic efficiency: The catalytic efficiency of the majority of current nanozymes remains inferior to that of natural enzymes. It is anticipated that diatomic and monoatomic nanozymes will enhance the catalytic efficiency of nanozymes. Furthermore, the activity of nanozymes is constrained by intricate TME, and the design of multifactorial responsive nanozymes will enhance the enzyme activity.

(III) Cascade catalysis: It is possible that a nano-enzyme with several enzymatic activities at the same time may exhibit synergistic effects in the anti-tumor process. Therefore, it is therefore of great importance to elucidate the sequence and comprehensiveness of the catalytic cascade catalyzed by multiple enzymes.

(IV) Biosecurity: The majority of current toxicity studies of nanozymes are limited to short-term cytotoxicity and in vivo toxicity assessments. The potential toxicity and clearance of nanozymes for long-term metabolism may limit their wide application.

(V) Single atom: SAzyme have been demonstrated to exhibit remarkable catalytic activity. However, further evaluation of their toxicity and stability is necessary.

(VI) Scope of application: Most of the research in the field of nanozymes has focused on the study of oxidoreductase and hydrolase activities. Other enzyme activities, such as transferase and lyase, have yet to be extensively investigated. Future work should explore the potential of nanozymes to mimic the activities of other enzymes for various applications.

(VII) Carrier:The fabrication of nanosystems with commendable biocompatibility, excellent targeting efficiency and multifaceted functionality is achieved through the grafting of tiny NPs onto suitable carriers.

(VIII) Mechanism research: The prevailing hypothesis is that the catalytic effect of nanozymes is primarily attributable to the metal ions they release. It is of great importance to conduct further theoretical studies in order to gain a more comprehensive understanding of the complete mechanism of nanozymes.

(IX) Targeted therapies: Exploring targeted therapies with low side effects, high precision and strong targeting, and synergising with other therapies to promote the development of individualised medicine is a trend for future research.

Acknowledgment

Ruilong Sun is the first author. Bo Fan and Li Songkai are Co-corresponding authors.

Funding

1. Plan G Talent Project (second stage), 2024-G2-2, The 940 hospital of the Joint Logistics Support Force of the Chinese People's Liberation Army. 2. General Project on Teaching Research and Reform in postgraduate education 2024, YBXM-202415, Gansu University of Chinese Medicine. 3. Longyuan young talents in Gansu Province.

Disclosure

The authors report no conflicts of interest in this work.

References

1. Ferlay J, Colombet M, Soerjomataram I, et al. Cancer statistics for the year 2020: an overview. *Int J Cancer*. 2021;149(4):778–789. doi:10.1002/ijc.33588
2. Riggio AI, Varley KE, Welm AL. The lingering mysteries of metastatic recurrence in breast cancer. *Br J Cancer*. 2021;124(1):13–26. doi:10.1038/s41416-020-01161-4
3. Bukowski K, Kciuk M, Kontek R. Mechanisms of multidrug resistance in cancer chemotherapy. *Int J mol Sci*. 2020;21(9):3233. doi:10.3390/ijms21093233
4. Nasir A, Khan A, Li J, et al. Nanotechnology, A tool for diagnostics and treatment of cancer. *Curr Top Med Chem*. 2021;21(15):1360–1376. doi:10.2174/1568026621666210701144124
5. GUGENHEIM J, CROVETTO A, PETRUCCIANI N. Neoadjuvant therapy for pancreatic cancer. *Updates Surg*. 2022;74(1):35–42. doi:10.1007/s13304-021-01186-1
6. Di Nardo P, Lisanti C, Garutti M, et al. Chemotherapy in patients with early breast cancer: clinical overview and management of long-term side effects. *Expert Opin Drug Saf*. 2022;21(11):1341–1355. doi:10.1080/14740338.2022.2151584

7. Wang K, Tepper JE. Radiation therapy-associated toxicity: etiology, management, and prevention. *CA Cancer J Clin*. 2021;71(5):437–454. doi:10.3322/caac.21689
8. LI Y, ZHAO L, LI XF. Hypoxia and the tumor microenvironment. *Technol Cancer Res Treat*. 2021;20:15330338211036304. doi:10.1177/15330338211036304
9. NIU B, Liao K, ZHOU Y, et al. Application of glutathione depletion in cancer therapy: enhanced ROS-based therapy, ferroptosis, and chemotherapy. *Biomaterials*. 2021;277:121110. doi:10.1016/j.biomaterials.2021.121110
10. Sun D, Pang X, Cheng Y, et al. Ultrasound-switchable nanozyme augments sonodynamic therapy against multidrug-resistant bacterial infection. *ACS Nano*. 2020;14(2):2063–2076. doi:10.1021/acsnano.9b08667
11. Li W, Qi M, Zhou J, et al. Pathogen-activated macrophage membrane encapsulated CeO(2) -TCPP nanozyme with targeted and photo-enhanced antibacterial therapy. *Small*. 2023;20:e2309664. doi:10.1002/smll.202309664
12. Zhang L, Li CX, Wan SS, et al. Nanocatalyst-mediated chemodynamic tumor therapy. *Adv Healthc Mater*. 2022;11(2):e2101971. doi:10.1002/adhm.202101971
13. Jia C, Guo Y, Wu FG. Chemodynamic therapy via fenton and fenton-like nanomaterials: strategies and recent advances. *Small*. 2022;18(6):e2103868. doi:10.1002/smll.202103868
14. YANG YC, ZHU Y, SUN SJ, et al. ROS regulation in gliomas: implications for treatment strategies. *Front Immunol*. 2023;14:1259797. doi:10.3389/fimmu.2023.1259797
15. HUANG Y, REN J, QU X. Nanozymes: classification, catalytic mechanisms, activity regulation, and applications. *Chem Rev*. 2019;119(6):4357–4412. doi:10.1021/acs.chemrev.8b00672
16. ZHANG Y, JIN Y, CUI H, et al. Nanozyme-based catalytic theranostics. *RSC Adv*. 2019;10(1):10–20. doi:10.1039/C9RA09021E
17. Matés JM, Campos-Sandoval JA, De Los Santos-Jiménez J, et al. Glutaminases regulate glutathione and oxidative stress in cancer. *Arch Toxicol*. 2020;94(8):2603–2623. doi:10.1007/s00204-020-02838-8
18. Wang L, Wang H. The putative role of ferroptosis in gastric cancer: a review. *Eur J Cancer Prev*. 2023;32(6):575–583. doi:10.1097/CEJ.0000000000000817
19. Cui YX, Park SH, Park WH. Anti-cancer effects of auranofin in human lung cancer cells by increasing intracellular ROS levels and depleting GSH levels. *Molecules*. 2022;27(16):5207. doi:10.3390/molecules27165207
20. Dong S, Dong Y, Jia T, et al. GSH-depleted nanozymes with hyperthermia-enhanced dual enzyme-mimic activities for tumor nanocatalytic therapy. *Adv Mater*. 2020;32(42):e2002439. doi:10.1002/adma.202002439
21. MAO H, WEN Y, YU Y, et al. Bioinspired nanocatalytic tumor therapy by simultaneous reactive oxygen species generation enhancement and glutamine pathway-mediated glutathione depletion. *J Mater Chem B*. 2022;11(1):131–143. doi:10.1039/D2TB02194C
22. LI D, HA E, ZHOU Z, et al. "Spark" PtMnIr nanozymes for electrodynamic-boosted multienzymatic tumor immunotherapy. *Adv Mater*. 2023;36:e2308747. doi:10.1002/adma.202308747
23. Wu F, Du Y, Yang J, et al. Peroxidase-like active nanomedicine with dual glutathione depletion property to restore oxaliplatin chemosensitivity and promote programmed cell death. *ACS Nano*. 2022;16(3):3647–3663. doi:10.1021/acsnano.1c06777
24. Zeng W, Liu C, Wang S, et al. SnFe(2)O(4) nanozyme based TME improvement system for anti-cancer combination thermoradiotherapy. *Front Oncol*. 2021;11:768829. doi:10.3389/fonc.2021.768829
25. Xu Y, Li Y, Li J, et al. Ethyl carbamate triggers ferroptosis in liver through inhibiting GSH synthesis and suppressing Nrf2 activation. *Redox Biol*. 2022;53:102349. doi:10.1016/j.redox.2022.102349
26. Qiu Y, Cao Y, Cao W, et al. The Application of Ferroptosis in Diseases. *Pharmacol Res*. 2020;159:104919. doi:10.1016/j.phrs.2020.104919
27. Sindhu RK, Najda A, Kaur P, et al. Potentiality of nanoenzymes for cancer treatment and other diseases: current status and future challenges. *Materials (Basel)*. 2021;14(20). doi:10.3390/ma14205965.
28. Jiang B, Guo Z, Liang M. Recent progress in single-atom nanozymes research. *Nano Res*. 2023;16(2):1878–1889. doi:10.1007/s12274-022-4856-7
29. Ashrafi AM, Bytesnikova Z, Barek J, et al. A critical comparison of natural enzymes and nanozymes in biosensing and bioassays. *Biosens Bioelectron*. 2021;192:113494. doi:10.1016/j.bios.2021.113494
30. Gao L, Zhuang J, Nie L, et al. Intrinsic peroxidase-like activity of ferromagnetic nanoparticles. *Nat Nanotechnol*. 2007;2(9):577–583. doi:10.1038/nnano.2007.260
31. Wu J, Wang X, Wang Q, et al. Nanomaterials with enzyme-like characteristics (nanozymes): next-generation artificial enzymes (II). *Chem Soc Rev*. 2019;48(4):1004–1076. doi:10.1039/c8cs00457a
32. Ren X, Chen D, Wang Y, et al. Nanozymes-recent development and biomedical applications. *J Nanobiotechnology*. 2022;20(1):92. doi:10.1186/s12951-022-01295-y
33. Gao L, Wei H, Dong S, et al. Nanozymes. *Adv Mater*. 2024;36(10):e2305249. doi:10.1002/adma.202305249
34. Zhang R, Fan K, Yan X. Nanozymes: created by learning from nature. *Sci China Life Sci*. 2020;63(8):1183–1200. doi:10.1007/s11427-019-1570-7
35. WU Y, DARLAND DC, ZHAO JX. Nanozymes-hitting the biosensing "Target". *Sensors*. 2021;21(15):1.
36. Wang Q, Jiang J, Gao L. Catalytic antimicrobial therapy using nanozymes. *Wiley Interdiscip Rev Nanomed Nanobiotechnol*. 2022;14(2):e1769. doi:10.1002/wnan.1769
37. Niu X, Liu B, Hu P, et al. Nanozymes with multiple activities: prospects in analytical sensing. *Biosensors*. 2022;12(4). doi:10.3390/bios12040251.
38. Chen Z, Yu Y, Gao Y, et al. Rational design strategies for nanozymes. *ACS Nano*. 2023;17(14):13062–13080. doi:10.1021/acsnano.3c04378
39. Tufail MA, Iltaf J, Zaheer T, et al. Recent advances in bioremediation of heavy metals and persistent organic pollutants: a review. *Sci Total Environ*. 2022;850:157961. doi:10.1016/j.scitotenv.2022.157961
40. Wang P, Min D, Chen G, et al. Inorganic nanozymes: prospects for disease treatments and detection applications. *Front Chem*. 2021;9:773285. doi:10.3389/fchem.2021.773285
41. Liu X, Gao Y, Chandrawati R, et al. Therapeutic applications of multifunctional nanozymes. *Nanoscale*. 2019;11(44):21046–21060. doi:10.1039/C9NR06596B

42. Chakraborty N, Gandhi S, Verma R, et al. Emerging prospects of nanozymes for antibacterial and anticancer applications. *Biomedicines*. 2022;10(6):1378. doi:10.3390/biomedicines10061378
43. Song N, YU Y, Zhang Y, et al. Bioinspired hierarchical self-assembled nanozyme for efficient antibacterial treatment. *Adv Mater*. 2024;36(10): e2210455. doi:10.1002/adma.202210455
44. B Liu, Wang Y, Chen Y, et al. Biomimetic two-dimensional nanozymes: synthesis, hybridization, functional tailoring, and biosensor applications. *J Mater Chem B*. 2020;8(44):10065–10086. doi:10.1039/D0TB02051F
45. Vokhmyanina DV, Andreeva KD, Komkova MA, et al. 'Artificial peroxidase' nanozyme - enzyme based lactate biosensor. *Talanta*. 2020;208:120393. doi:10.1016/j.talanta.2019.120393
46. Guo QJ, Pan ZY, Men C, et al. Visual detection of cancer cells by using in situ grown functional Cu 2−x Se/reduced graphene oxide hybrids acting as an efficient nanozyme. *Analyst*. 2019;144(2):716–721. doi:10.1039/C8AN01849A
47. N PN, Mehla S, Begum A, et al. Smart nanozymes for cancer therapy: the next frontier in oncology. *Adv Healthc Mater*. 2023;12(25):e2300768. doi:10.1002/adhm.202300768
48. ZHANG A, GAO A, ZHOU C, et al. Confining prepared ultrasmall nanozymes loading ATO for lung cancer catalytic therapy/immunotherapy. *Adv Mater*. 2023;35(45):e2303722. doi:10.1002/adma.202303722
49. YAO H, ZHOU R, WANG J, et al. Pathogen-targeting bimetallic nanozymes as ultrasonic-augmented ros generator against multidrug resistant bacterial infection. *Adv Healthc Mater*. 2023;12(25):e2300449. doi:10.1002/adhm.202300449
50. Xiang K, Wu H, Liu Y, et al. MOF-derived bimetallic nanozyme to catalyze ROS scavenging for protection of myocardial injury. *Theranostics*. 2023;13(8):2721–2733. doi:10.7150/thno.83543
51. Li Q, Liu Y, Dai X, et al. Nanozymes regulate redox homeostasis in ros-related inflammation. *Front Chem*. 2021;9:740607. doi:10.3389/fchem.2021.740607
52. Gao F, Shao T, Yu Y, et al. Surface-bound reactive oxygen species generating nanozymes for selective antibacterial action. *Nat Commun*. 2021;12(1):745. doi:10.1038/s41467-021-20965-3
53. Singh S. Antioxidant nanozymes as next-generation therapeutics to free radical-mediated inflammatory diseases: a comprehensive review. *Int J Biol Macromol*. 2024;260(Pt 1):129374. doi:10.1016/j.ijbiomac.2024.129374
54. Mehta D, Singh S. Nanozymes and their biomolecular conjugates as next-generation antibacterial agents: a comprehensive review. *Int J Biol Macromol*. 2024;278(Pt 1):134582. doi:10.1016/j.ijbiomac.2024.134582
55. Zhang Y, Zhang N, Gong SP, et al. Nanozyme-based synergistic therapeutic strategies against tumors. *Drug Discov Today*. 2025;30(2):104292. doi:10.1016/j.drudis.2025.104292
56. Albalawi AE, Khalaf KA, Alyousif MS, et al. Fe3O4(@)piroctone olamine magnetic nanoparticles: synthesize and therapeutic potential in cutaneous leishmaniasis. *Biomed Pharmacother*. 2021;139:111566. doi:10.1016/j.biopha.2021.111566
57. Zhang H, Wang T, Liu H, et al. Second near-infrared photodynamic therapy and chemotherapy of orthotopic malignant glioblastoma with ultra-small Cu(2-x)Se nanoparticles. *Nanoscale*. 2019;11(16):7600–7608. doi:10.1039/C9NR01789E
58. Siddiqi SK, Husen A, Rao RAK. A review on biosynthesis of silver nanoparticles and their biocidal properties. *J Nanobiotechnology*. 2018;16 (1):14. doi:10.1186/s12951-018-0334-5
59. Xu K, Wu X, Cheng Y, et al. A biomimetic nanoenzyme for starvation therapy enhanced photothermal and chemodynamic tumor therapy. *Nanoscale*. 2020;12(45):23159–23165. doi:10.1039/D0NR05097K
60. Tian R, Sun J, Qi Y, et al. Influence of VO_2 nanoparticle morphology on the colorimetric assay of H_2O_2 and glucose. *Nanomaterials (Basel)*. 2017;7(11). doi:10.3390/nano7110347.
61. Zhou Y, lei H, Wang M, et al. Potent intrinsic bactericidal activity of novel copper telluride nano-grape clusters with facile preparation. *Biomater Sci*. 2023;11(5):1828–1839. doi:10.1039/D2BM01617F
62. YAN H, Dong J, Luan X, et al. Ultrathin porous nitrogen-doped carbon-coated cuse heterostructures for combination cancer therapy of photothermal therapy, photocatalytic therapy, and logic-gated chemotherapy. *ACS Appl Mater Interfaces*. 2022;14(50):56237–56252. doi:10.1021/acsami.2c12503
63. Jiang C, Shi Q, Yang J, et al. Ceria nanozyme coordination with curcumin for treatment of sepsis-induced cardiac injury by inhibiting ferroptosis and inflammation. *J Adv Res*. 2024;63:159–170. doi:10.1016/j.jare.2023.10.011
64. Lu J, Mao Y, Feng S, et al. Biomimetic smart mesoporous carbon nanozyme as a dual-GSH depletion agent and O(2) generator for enhanced photodynamic therapy. *Acta Biomater*. 2022;148:310–322. doi:10.1016/j.actbio.2022.06.001
65. LIU Y, AI K, JI X, et al. Comprehensive insights into the multi-antioxidative mechanisms of melanin nanoparticles and their application to protect brain from injury in ischemic stroke. *J Am Chem Soc*. 2017;139(2):856–862. doi:10.1021/jacs.6b11013
66. Kalinina EV, gavriliuk LA. Glutathione synthesis in cancer cells. *Biochemistry*. 2020;85(8):895–907. doi:10.1134/S0006297920080052
67. SUN X, GUO F, YE Q, et al. Fluorescent SENSING OF GLUTATHIONE AND RELATED BIO-APPLications. *Biosensors (Basel)*. 2022;13 (1). doi:10.3390/bios13010016.
68. Georgiou-Siafis SK, Tsiftsoglou AS. the key role of gsh in keeping the redox balance in mammalian cells: mechanisms and significance of gsh in detoxification via formation of conjugates. *Antioxidants (Basel)*. 2023;12(11). doi:10.3390/antiox12111953
69. Fraternale A, Paoletti MF, Casabianca A, et al. GSH and analogs in antiviral therapy. *mol Aspects Med*. 2009;30(1–2):99–110. doi:10.1016/j.mam.2008.09.001
70. Elia I, Haigis MC. Metabolites and the tumour microenvironment: from cellular mechanisms to systemic metabolism. *Nat Metab*. 2021;3 (1):21–32. doi:10.1038/s42255-020-00317-z
71. Singh R, Karakoti AS, Self W, et al. Redox-sensitive cerium oxide nanoparticles protect human keratinocytes from oxidative stress induced by glutathione depletion. *Langmuir*. 2016;32(46):12202–12211. doi:10.1021/acs.langmuir.6b03022
72. Meng X, Li D, Chen L, et al. High-performance self-cascade pyrite nanozymes for apoptosis-ferroptosis synergistic tumor therapy. *ACS Nano*. 2021;15(3):5735–5751. doi:10.1021/acsnano.1c01248
73. Zhu L, dai Y, Gao L, et al. Tumor microenvironment-modulated nanozymes for NIR-II-triggered hyperthermia-enhanced photo-nanocatalytic therapy via disrupting ROS homeostasis. *Int J Nanomedicine*. 2021;16:4559–4577. doi:10.2147/IJN.S309062
74. Li S, Ding H, Chang J, et al. Bimetallic oxide nanozyme-mediated depletion of glutathione to boost oxidative stress for combined nanocatalytic therapy. *J Colloid Interface Sci*. 2022;623:787–798. doi:10.1016/j.jcis.2022.05.059

75. S LIU, LI W, DING H, et al. Biomineralized RuO(2) nanozyme with multi-enzyme activity for ultrasound-triggered peroxynitrite-boosted ferroptosis. *Small*. 2023;19(45):e2303057. doi:10.1002/smll.202303057
76. HAN D, DING B, ZHENG P, et al. NADPH oxidase-like nanozyme for high-efficiency tumor therapy through increasing glutathione consumption and blocking glutathione regeneration. *Adv Healthc Mater*. 2024;13(11):e2303309. doi:10.1002/adhm.202303309
77. Phan NM, Nguyen TL, Kim J. Nanozyme-based enhanced cancer immunotherapy. *Tissue Eng Regen Med*. 2022;19(2):237–252. doi:10.1007/s13770-022-00430-y
78. XIONG Y, Mi B, Liu G, et al. Microenvironment-sensitive nanozymes for tissue regeneration. *Biomaterials*. 2024;309:122585. doi:10.1016/j.biomaterials.2024.122585
79. Xiao Y, Yu D. Tumor microenvironment as a therapeutic target in cancer. *Pharmacol Ther*. 2021;221:107753. doi:10.1016/j.pharmthera.2020.107753
80. Liu G, Liu M, Li X, et al. Peroxide-simulating and GSH-depleting nanozyme for enhanced chemodynamic/photodynamic therapy via induction of multisource ROS. *ACS Appl Mater Interfaces*. 2023;15(41):47955–47968. doi:10.1021/acsami.3c09873
81. Liu T, Sun L, Zhang Y, et al. Imbalanced GSH/ROS and sequential cell death. *J Biochem mol Toxicol*. 2022;36(1):e22942. doi:10.1002/jbt.22942
82. Wang S, Zhang Q, Zeng N, et al. Injectable hydrogel system for camptothecin initiated nanocatalytic tumor therapy with high performance. *Front Oncol*. 2022;12:904960. doi:10.3389/fonc.2022.904960
83. Huang C, Liu Z, Chen M, et al. Tumor-derived biomimetic nanozyme with immune evasion ability for synergistically enhanced low dose radiotherapy. *J Nanobiotechnology*. 2021;19(1):457. doi:10.1186/s12951-021-01182-y
84. Chen Y, Lin J, Pan Q, et al. Inter-metal interaction of dual-atom catalysts in heterogeneous catalysis. *Angew Chem Int Ed Engl*. 2023;62(42):e202306469. doi:10.1002/anie.202306469
85. Li T, Gu Y, Yu L, et al. Stimuli-responsive double single-atom catalysts for parallel catalytic therapy. *Pharmaceutics*. 2023;15(4):1217. doi:10.3390/pharmaceutics15041217
86. Liu Y, Niu R, Deng R, et al. Multi-enzyme Co-expressed dual-atom nanozymes induce cascade immunogenic ferroptosis via activating interferon-γ and targeting arachidonic acid metabolism. *J Am Chem Soc*. 2023;145(16):8965–8978. doi:10.1021/jacs.2c13689
87. Rong M, Liu J, Lu L. Self-assembly of 2D polyphthalocyanine in lysosome enables multienzyme activity enhancement to induce tumor ferroptosis. *Adv Healthc Mater*. 2024;13(15):e2400325. doi:10.1002/adhm.202400325
88. Fu S, Li Y, Shen L, et al. Cu 2 WS 4 -PEG nanozyme as multifunctional sensitizers for enhancing immuno-radiotherapy by inducing ferroptosis. *Small*. 2024;20:e2309537. doi:10.1002/smll.202309537
89. Chen W, Xie W, Gao Z, et al. Mild-photothermal effect induced high efficiency ferroptosis-boosted-cuproptosis based on Cu(2) O@Mn(3) Cu (3) O(8) nanozyme. *Adv Sci (Weinh)*. 2023;10(33):e2303694. doi:10.1002/advs.202303694
90. Zhang J, Ha E, Li D, et al. Dual enzyme-like Co-FeSe(2) nanoflowers with GSH degradation capability for NIR II-enhanced catalytic tumor therapy. *J Mater Chem B*. 2023;11(19):4274–4286. doi:10.1039/D3TB00220A
91. He L, Ji Q, Chi B, et al. Construction nanoenzymes with elaborately regulated multi-enzymatic activities for photothermal-enhanced catalytic therapy of tumor. *Colloids Surf B Biointerfaces*. 2023;222:113058. doi:10.1016/j.colsurfb.2022.113058
92. Wang TH, Shen MY, Yeh NT, et al. Photothermal nanozymes to self-augment combination cancer therapy by dual-glutathione depletion and hyperthermia/acidity-activated hydroxyl radical generation. *J Colloid Interface Sci*. 2023;650(Pt B):1698–1714. doi:10.1016/j.jcis.2023.07.134
93. Wang Z, Liu B, Sun Q, et al. Upconverted metal-organic framework janus architecture for near-infrared and ultrasound co-enhanced high performance tumor therapy. *ACS Nano*. 2021;15(7):12342–12357. doi:10.1021/acsnano.1c04280
94. HU Y, Wang K, Ye C. "four-in-one" nanozyme and natural enzyme symbiotic system of Cu(2-x) Se-GOx for cervical cancer therapy. *Chemistry*. 2022;28(1):e202102885. doi:10.1002/chem.202102885
95. Guo B, Yang F, ZHANG L, et al. Cuproptosis Induced by ROS responsive nanoparticles with elesclomol and copper combined with αPD-l1 for enhanced cancer immunotherapy. *Adv Mater*. 2023;35(22):e2212267. doi:10.1002/adma.202212267
96. Wang X, Shi Q, Zha Z, et al. Copper single-atom catalysts with photothermal performance and enhanced nanozyme activity for bacteria-infected wound therapy. *Bioact Mater*. 2021;6(12):4389–4401. doi:10.1016/j.bioactmat.2021.04.024
97. Zhang W, Wang M, Liu B, et al. Glutathione induced in situ synthesis of cu single-atom nanozymes with anaerobic glycolysis metabolism interference for boosting cuproptosis. *Angew Chem Int Ed Engl*. 2024;63(18):e202402397. doi:10.1002/anie.202402397
98. Guan X, Ge X, Dong H, et al. Ultrathin 2D Pd/Cu single-atom MOF nanozyme to synergistically overcome chemoresistance for multienzyme catalytic cancer therapy. *Adv Healthc Mater*. 2023;12(30):e2301853. doi:10.1002/adhm.202301853
99. Chen J, Liu X, Zheng G, et al. Detection of glucose based on noble metal nanozymes: mechanism, activity regulation, and enantioselective recognition. *Small*. 2023;19(8):e2205924. doi:10.1002/smll.202205924
100. Wang Q, Liu J, He L, et al. Nanozyme: a rising star for cancer therapy. *Nanoscale*. 2023;15(30):12455–12463. doi:10.1039/D3NR01976D
101. Filik H, Avan AA, Tokatli ZF. A review on colorimetric sensing of tumor markers based on enzyme-mimicking nanomaterials. *Curr Med Chem*. 2021;28(30):6123–6145. doi:10.2174/0929867328666210412122604
102. Zhao DH, Li CQ, Hou XL, et al. Tumor microenvironment-activated theranostics nanozymes for fluorescence imaging and enhanced chemo-chemodynamic therapy of tumors. *ACS Appl Mater Interfaces*. 2021;13(47):55780–55789. doi:10.1021/acsami.1c12611
103. Wu F, Chen H, Liu R, et al. Modulation of the tumor immune microenvironment by Bi(2) Te(3) -au/pd-based theranostic nanocatalysts enables efficient cancer therapy. *Adv Healthc Mater*. 2022;11(19):e2200809. doi:10.1002/adhm.202200809
104. Tu L, Chen S, Yuan Z, et al. Amino acid-based metallo-supramolecular nanoassemblies capable of regulating cellular redox homeostasis for tumoricidal chemo-/photo-/catalytic combination therapy. *J Colloid Interface Sci*. 2024;663:810–824. doi:10.1016/j.jcis.2024.02.197
105. Zhang L, Dong Q, Hao Y, et al. Drug-primed self-assembly of platinum-single-atom nanozyme to regulate cellular redox homeostasis against cancer. *Adv Sci*. 2023;10(30):e2302703. doi:10.1002/advs.202302703
106. Pan MM, Li P, Yu YP, et al. Bimetallic ions functionalized metal-organic-framework nanozyme for tumor microenvironment regulating and enhanced photodynamic therapy for hypoxic tumor. *Adv Healthc Mater*. 2023;12(26):e2300821. doi:10.1002/adhm.202300821
107. Dugan LL, Turetsky DM, Du C, et al. Carboxyfullerenes as neuroprotective agents. *Proc Natl Acad Sci U S A*. 1997;94(17):9434–9439. doi:10.1073/pnas.94.17.9434

108. Rasras S, Kalantari H, Rezaei M, et al. Single-walled and multiwalled carbon nanotubes induce oxidative stress in isolated rat brain mitochondria. *Toxicol Ind Health*. 2019;35(7):497–506. doi:10.1177/0748233719856983
109. Nasim I, Ghani N, Nawaz R, et al. Investigating the impact of carbon nanotube nanoparticle exposure on testicular oxidative stress and histopathological changes in Swiss albino mice. *ACS Omega*. 2024;9(6):6731–6740. doi:10.1021/acsomega.3c07919
110. Yao L, Zhao MM, Luo QW, et al. Carbon quantum dots-based nanozyme from coffee induces cancer cell ferroptosis to activate antitumor immunity. *ACS Nano*. 2022;16(6):9228–9239. doi:10.1021/acsnano.2c01619
111. Yu H, Tang K, Cai Z, et al. Carbon dots-based nanozyme for drug-resistant lung cancer therapy by encapsulated doxorubicin/siRNA cocktail. *Int J Nanomedicine*. 2023;18:933–948. doi:10.2147/IJN.S390984
112. Hu C, Dai L. Doping of carbon materials for metal-free electrocatalysis. *Adv Mater*. 2019;31(7):e1804672. doi:10.1002/adma.201804672
113. Geng B, XU S, Li P, et al. Platinum crosslinked carbon Dot@TiO(2-)(x) p-n junctions for relapse-free sonodynamic tumor eradication via high-yield ROS and GSH depletion. *Small*. 2022;18(6):e2103528. doi:10.1002/smll.202103528
114. Zhou M, Yang Z, Yin T, et al. Functionalized Fe-doped carbon dots exhibiting dual glutathione consumption to amplify ferroptosis for enhanced cancer therapy. *ACS Appl Mater Interfaces*. 2023;15(46):53228–53241. doi:10.1021/acsami.3c12356
115. Nie Y, Li D, Peng Y, et al. Metal organic framework coated MnO(2) nanosheets delivering doxorubicin and self-activated DNAzyme for chemo-gene combinatorial treatment of cancer. *Int J Pharm*. 2020;585:119513. doi:10.1016/j.ijpharm.2020.119513
116. Wu A, Han M, Ni Z, et al. Multifunctional Sr/Se co-doped ZIF-8 nanozyme for chemo/chemodynamic synergistic tumor therapy via apoptosis and ferroptosis. *Theranostics*. 2024;14(5):1939–1955. doi:10.7150/thno.92663
117. Liu B, Wang X, Chen X, et al. Au(I)-incorporated metal-organic frameworks nanozymes for thioreduction and glutathione depletion-mediated efficient photoimmunotherapy. *J Colloid Interface Sci*. 2025;683(Pt 1):552–563. doi:10.1016/j.jcis.2024.12.057
118. Yao C, Zhang R, Xie Z, et al. A Magnetically Actuated MOF-Based Nanozyme for Intensified Induction of Ferroptosis and Immunogenic Cell Death Via Autophagy Blockade. *Small*. 2025;21(5):e2409026. doi:10.1002/smll.202409026
119. Zhu X, Liu Y, Yuan G, et al. In situ fabrication of MS@MnO(2) hybrid as nanozymes for enhancing ROS-mediated breast cancer therapy. *Nanoscale*. 2020;12(43):22317–22329. doi:10.1039/D0NR03931D
120. Ye J, Zhang K, Yang X, et al. Embedding atomically dispersed manganese/gadolinium dual sites in oxygen vacancy-enriched biodegradable bimetallic silicate nanoplatform for potentiating catalytic therapy. *Adv Sci*. 2024;11(4):e2307424. doi:10.1002/advs.202307424
121. Lv W, CAO M, LIU J, et al. Tumor microenvironment-responsive nanozymes achieve photothermal-enhanced multiple catalysis against tumor hypoxia. *Acta Biomater*. 2021;135:617–627. doi:10.1016/j.actbio.2021.08.015
122. Li L, Lin Z, Xu X, et al. A pH/GSH/glucose responsive nanozyme for tumor cascade amplified starvation and chemodynamic theranostics. *ACS Appl Mater Interfaces*. 2023;15(35):41224–41236. doi:10.1021/acsami.3c05412
123. Hu D, Li D, Liu X, et al. Vanadium-based nanomaterials for cancer diagnosis and treatment. *Biomed Mater*. 2020;16(1):014101. doi:10.1088/1748-605X/abb523
124. Zeng X, Wang H, Ma Y, et al. Vanadium oxide nanozymes with multiple enzyme-mimic activities for tumor catalytic therapy. *ACS Appl Mater Interfaces*. 2023;2023:1.
125. WANG Y, ZHANG R, ZANG P, et al. Synergizing pyroelectric catalysis and enzyme catalysis: establishing a reciprocal and synergistic model to enhance anti-tumor activity. *Adv Mater*. 2024;36(24):e2401111. doi:10.1002/adma.202401111
126. Zhong S, Zhang Z, Zhao Y, et al. Bismuth nanoclusters on nitrogen-doped porous carbon nanoenzyme for cancer therapy. *Nanoscale*. 2023;15(41):16619–16625. doi:10.1039/D3NR03957A
127. Ren G, Lu M, Zhao Z, et al. Cobalt Single-Atom Nanozyme Co-Administration with Ascorbic Acid Enables Redox Imbalance for Tumor Catalytic Ablation. *ACS Biomater Sci Eng*. 2023;9(2):1066–1076. doi:10.1021/acsbiomaterials.2c01301
128. Wang L, Zhang X, You Z, et al. A molybdenum disulfide nanozyme with charge-enhanced activity for ultrasound-mediated cascade-catalytic tumor ferroptosis. *Angew Chem Int Ed Engl*. 2023;62(11):e202217448. doi:10.1002/anie.202217448
129. Wang Q, Shaik F, Lu X, et al. Amorphous NiB@IrO(x) nanozymes trigger efficient apoptosis-ferroptosis hybrid therapy. *Acta Biomater*. 2023;155:575–587. doi:10.1016/j.actbio.2022.10.048
130. Jefferies H, Coster J, Khalil A, et al. Glutathione. *ANZ J Surg*. 2003;73(7):517–522. doi:10.1046/j.1445-1433.2003.02682.x
131. FENG S, WANG J, MU X, et al. Mesoporous carbon nanoenzyme as nano-booster for photothermal-enhanced photodynamic therapy compared with graphene oxide. *Colloids Surf B Biointerfaces*. 2023;222:113095. doi:10.1016/j.colsurfb.2022.113095
132. Yan L, Shang S, Hu J, et al. An NIR-II-photoresponsive CoSnO(3) nanozyme for mild photothermally augmented nanocatalytic cancer therapy. *J Mater Chem B*. 2024;12(3):710–719. doi:10.1039/D3TB02018E
133. Li D, Ha E, Zhou Z, et al. "Spark" PtMnIr nanozymes for electrodynamic-boosted multienzymatic tumor immunotherapy. *Adv Mater*. 2024;36(13):e2308747.
134. Su Y, Lv M, Huang Z, et al. Defect engineering to tailor structure-activity relationship in biodegradable nanozymes for tumor therapy by dual-channel death strategies. *J Control Release*. 2024;367:557–571. doi:10.1016/j.jconrel.2024.01.066
135. Wei L, Wang Z, Lu X, et al. Interfacial strong interaction-enabling cascade nanozymes for apoptosis-ferroptosis synergistic therapy. *J Colloid Interface Sci*. 2024;653(Pt A):20–29. doi:10.1016/j.jcis.2023.09.036
136. Ying M, You D, Zhu X, et al. Lactate and glutamine support NADPH generation in cancer cells under glucose deprived conditions. *Redox Biol*. 2021;46:102065. doi:10.1016/j.redox.2021.102065
137. Zhang D, Hua Z, Li Z. The role of glutamate and glutamine metabolism and related transporters in nerve cells. *CNS Neurosci Ther*. 2024;30(2):e14617. doi:10.1111/cns.14617
138. Averill-Bates DA. The antioxidant glutathione. *Vitam Horm*. 2023;121:109–141.
139. Sharma P, Aaroe A, Liang J, et al. Tumor microenvironment in glioblastoma: current and emerging concepts. *Neurooncol Adv*. 2023;5(1):vdad009. doi:10.1093/noajnl/vdad009
140. Lasorsa F, Rutigliano M, Milella M, et al. Cellular and molecular players in the tumor microenvironment of renal cell carcinoma. *J Clin Med*. 2023;12(12):3888. doi:10.3390/jcm12123888
141. Xu J, Tang X, Yang X, et al. pH and GSH dual-responsive drug-controlled nanomicelles for breast cancer treatment. *Biomed Mater*. 2023;18(2):025021. doi:10.1088/1748-605X/acb7bb

142. Zhang Z, Ding D, Liu J, et al. Supramolecular nanozyme system based on polydopamine and polyoxometalate for photothermal-enhanced multienzyme cascade catalytic tumor therapy. *ACS Appl Mater Interfaces*. 2023;15(32):38214–38229. doi:10.1021/acsami.3c04723
143. Wang YY, Zhang XY, Li SL, et al. AuPt-loaded cu-doped polydopamine nanocomposites with multienzyme-mimic activities for dual-modal imaging-guided and cuproptosis-enhanced photothermal/nanocatalytic therapy. *Anal Chem*. 2023;95(37):14025–14035. doi:10.1021/acs.analchem.3c02661
144. Xie W, Gan Y, Wang L, et al. Tumor microenvironment-activated nanostructure to enhance MRI capability and nanozyme activity for highly tumor-specific multimodal theranostics. *Small*. 2024;20(14):e2306446. doi:10.1002/smll.202306446
145. Yang P, Tao J, Chen F, et al. Multienzyme-mimic ultrafine alloyed nanoparticles in metal organic frameworks for enhanced chemodynamic therapy. *Small*. 2021;17(7):e2005865. doi:10.1002/smll.202005865
146. Cui S, Wang B, Zhai C, et al. A double rare earth doped CD nanoplatform for nanocatalytic/starving-like synergistic therapy with GSH-depletion and enhanced reactive oxygen species generation. *J Mater Chem B*. 2023;11(33):7986–7997. doi:10.1039/D3TB00959A
147. Zhou Z, Gao Z, Chen W, et al. Nitric oxide-mediated regulation of mitochondrial protective autophagy for enhanced chemodynamic therapy based on mesoporous Mo-doped Cu(9)S(5) nanozymes. *Acta Biomater*. 2022;151:600–612. doi:10.1016/j.actbio.2022.08.011
148. Elhanani O, Ben-Uri R, Keren L. Spatial profiling technologies illuminate the tumor microenvironment. *Cancer Cell*. 2023;41(3):404–420. [J]. doi:10.1016/j.ccell.2023.01.010
149. Jin MZ, Jin WL. The updated landscape of tumor microenvironment and drug repurposing. *Signal Transduct Target Ther*. 2020;5(1):166. [J]. doi:10.1038/s41392-020-00280-x
150. Jarosz-Biej M, Smolarczyk R, cichoń T, et al. Tumor microenvironment as A "Game Changer" in cancer radiotherapy. *Int J mol Sci*. 2019;20(13):3212. doi:10.3390/ijms20133212
151. Bader JE, Voss K, Rathmell JC. Targeting metabolism to improve the tumor microenvironment for cancer immunotherapy. *Mol Cell*. 2020;78(6):1019–1033. [J]. doi:10.1016/j.molcel.2020.05.034
152. Zhang Z, Wang L, Guo Z, et al. A pH-sensitive imidazole grafted polymeric micelles nanoplatform based on ROS amplification for ferroptosis-enhanced chemodynamic therapy. *Colloids Surf B Biointerfaces*. 2024;237:113871. doi:10.1016/j.colsurfb.2024.113871
153. Zhang Z, Yue P, Lu T, et al. Role of lysosomes in physiological activities, diseases, and therapy. *J Hematol Oncol*. 2021;14(1):79.
154. Bhardwaj M, Lee JJ, Versace AM, et al. Lysosomal lipid peroxidation regulates tumor immunity. *J Clin Invest*. 2023;133(8). doi:10.1172/JCI164596.
155. Zhao L, Zhang X, Wang X, et al. Recent advances in selective photothermal therapy of tumor. *J Nanobiotechnol*. 2021;19(1):335. doi:10.1186/s12951-021-01080-3
156. Liu T, Zhu M, Chang X, et al. Tumor-specific photothermal-therapy-assisted immunomodulation via multiresponsive adjuvant nanoparticles. *Adv Mater*. 2023;35(18):e2300086. doi:10.1002/adma.202300086
157. Chen Q, Hu Q, Dukhovlinova E, et al. Photothermal therapy promotes tumor infiltration and antitumor activity of car t cells. *Adv Mater*. 2019;31(23):e1900192. doi:10.1002/adma.201900192
158. Wang F, Li J, Chen C, et al. Preparation and synergistic chemo-photothermal therapy of redox-responsive carboxymethyl cellulose/chitosan complex nanoparticles. *Carbohydr Polym*. 2022;275:118714. doi:10.1016/j.carbpol.2021.118714
159. Kumar AVP, Dubey SK, Tiwari S, et al. Recent advances in nanoparticles mediated photothermal therapy induced tumor regression. *Int J Pharm*. 2021;606:120848. doi:10.1016/j.ijpharm.2021.120848
160. Zheng J, Gao P. Toward normalization of the Tumor microenvironment for cancer therapy. *Integr Cancer Ther*. 2019;18:1534735419862352. doi:10.1177/1534735419862352
161. Xu Q, Lan X, Lin H, et al. Tumor microenvironment-regulating nanomedicine design to fight multi-drug resistant tumors. *Wiley Interdiscip Rev Nanomed Nanobiotechnol*. 2023;15(1):e1842. doi:10.1002/wnan.1842
162. zhuang J, Midgley AC, Wei Y, et al. Machine-learning-assisted nanozyme design: lessons from materials and engineered enzymes. *Adv Mater*. 2024;36(10):e2210848. doi:10.1002/adma.202210848
163. Wu Y, Tang Y, Xu W, et al. Photothermal-switched single-atom nanozyme specificity for pretreatment and sensing. *Small*. 2023;19(40):e2302929. doi:10.1002/smll.202302929
164. Ali S, Sikdar S, Basak S, et al. β-cyclodextrin-stabilized biosynthesis nanozyme for dual enzyme mimicking and Fenton reaction with a high potential anticancer agent. *ACS Omega*. 2022;7(5):4457–4470. doi:10.1021/acsomega.1c06322
165. Sun W, Zhu C, Song J, et al. Hydrogen sulfide gas amplified ros cascade: fes@gox hybrid nanozyme designed for boosting tumor chemodynamic immunotherapy. *Adv Healthc Mater*. 2023;12(23):e2300385. doi:10.1002/adhm.202300385
166. Wang Q, Niu D, Shi J, et al. A Three-in-one ZIFs-Derived CuCo(O)/GOx@PCNs Hybrid Cascade Nanozyme for Immunotherapy/Enhanced Starvation/Photothermal Therapy. *ACS Appl Mater Interfaces*. 2021;13(10):11683–11695. doi:10.1021/acsami.1c01006
167. Wang M, Chang M, Zheng P, et al. A noble AuPtAg-GOx nanozyme for synergistic tumor immunotherapy induced by starvation therapy-augmented mild photothermal therapy. *Adv Sci (Weinh)*. 2022;9(31):e2202332. doi:10.1002/advs.202202332
168. Qi P, Luo C, Pan Y, et al. Self-cascade catalytic single-atom nanozyme for enhanced breast cancer low-dose radiotherapy. *Colloids Surf B Biointerfaces*. 2023;227:113347. doi:10.1016/j.colsurfb.2023.113347
169. Cai X, Liu R, Yan H, et al. Cascaded nanozyme with in situ enhanced photothermal capacity for tumor-specific and self-replenishing cancer therapy. *Adv Healthc Mater*. 2023;12(27):e2300516. doi:10.1002/adhm.202300516
170. Wang M, Chang M, Li C, et al. Tumor-microenvironment-activated reactive oxygen species amplifier for enzymatic cascade cancer starvation/chemodynamic /immunotherapy. *Adv Mater*. 2022;34(4):e2106010. doi:10.1002/adma.202106010
171. Sun J, Zhao H, Xu W, et al. Recent advances in photothermal therapy-based multifunctional nanoplatforms for breast cancer. *Front Chem*. 2022;10:1024177. doi:10.3389/fchem.2022.1024177
172. Wang T, Xu X, Zhang K. Nanotechnology-enabled chemodynamic therapy and immunotherapy. *Curr Cancer Drug Targets*. 2021;21(7):545–557. doi:10.2174/1568009621666210219101552
173. Wu T, Liu Y, Cao Y, et al. Engineering macrophage exosome disguised biodegradable nanoplatform for enhanced sonodynamic therapy of glioblastoma. *Adv Mater*. 2022;34(15):e2110364. doi:10.1002/adma.202110364
174. Yu Z, Hu Y, Sun Y, et al. Chemodynamic therapy combined with multifunctional nanomaterials and their applications in tumor treatment. *Chemistry*. 2021;27(56):13953–13960. doi:10.1002/chem.202101514

175. Gao H, Cao Z, Liu H, et al. Multifunctional nanomedicines-enabled chemodynamic-synergized multimodal tumor therapy via Fenton and Fenton-like reactions. *Theranostics*. 2023;13(6):1974–2014. doi:10.7150/thno.80887
176. Hirsch LR, Stafford RJ, Bankson JA, et al. Nanoshell-mediated near-infrared thermal therapy of tumors under magnetic resonance guidance. *Proc Natl Acad Sci U S A*. 2003;100(23):13549–13554. doi:10.1073/pnas.2232479100
177. Zhi D, Yang T, O'hagan J, et al. Photothermal therapy. *J Control Release*. 2020;325:52–71. doi:10.1016/j.jconrel.2020.06.032
178. Zhang C, Guo J, Zou X, et al. Acridine-based covalent organic framework photosensitizer with broad-spectrum light absorption for antibacterial photocatalytic therapy. *Adv Healthc Mater*. 2021;10(19):e2100775. doi:10.1002/adhm.202100775
179. Xiao R, Zeng J, Li F, et al. Gold-semiconductor nanohybrids as advanced phototherapeutics. *Nanomedicine*. 2023;18(22):1585–1606. doi:10.2217/nnm-2023-0118
180. Wang Y, Xu Y, Song J, et al. Tumor cell-targeting and tumor microenvironment-responsive nanoplatforms for the multimodal imaging-guided photodynamic/photothermal/chemodynamic treatment of cervical cancer. *Int J Nanomedicine*. 2024;19:5837–5858. doi:10.2147/IJN.S466042
181. Mchale AP, Callan JF, Nomikou N, et al. Sonodynamic therapy: concept, mechanism and application to cancer treatment. *Adv Exp Med Biol*. 2016;880:429–450.
182. Hu H, Zhao J, Ma K, et al. Sonodynamic therapy combined with phototherapy: novel synergistic strategy with superior efficacy for antitumor and antiinfection therapy. *J Control Release*. 2023;359:188–205. doi:10.1016/j.jconrel.2023.05.041
183. Wang S, Zeng N, Zhang Q, et al. Nanozyme hydrogels for self-augmented sonodynamic/photothermal combination therapy. *Front Oncol*. 2022;12:888855. doi:10.3389/fonc.2022.888855
184. Dong Q, Jiang Z. Platinum–iron nanoparticles for oxygen-enhanced sonodynamic tumor cell suppression. *Inorganics*. 2024;12(12):331. doi:10.3390/inorganics12120331
185. Xiao X, Chen M, Zhang Y, et al. Hemin-incorporating DNA nanozyme enabling catalytic oxygenation and GSH depletion for enhanced photodynamic therapy and synergistic tumor ferroptosis. *J Nanobiotechnology*. 2022;20(1):410. doi:10.1186/s12951-022-01617-0
186. Zhu X, Zheng L, Zhao P, et al. Fe/Cu bimetallic nanozyme co-assembled with (177)Lu and Tanshinone for quadruple-synergistic tumor-specific therapy. *Adv Healthc Mater*. 2024;14:e2402696. doi:10.1002/adhm.202402696
187. Li X, Zhang Y, Liu A, et al. Nanozyme as tumor energy homeostasis disruptor mediated ferroptosis for high-efficiency radiotherapy. *J Colloid Interface Sci*. 2025;688:44–58. doi:10.1016/j.jcis.2025.02.125
188. Zhang N, Ping W, Xiang J, et al. Biomimetic single-atom nanozyme for dual starvation-enhanced breast cancer immunotherapy. *Adv Healthc Mater*. 2024;14:e2401362. doi:10.1002/adhm.202401362
189. Zhao L, Tong Y, Yin J, et al. Photo-activated oxidative stress amplifier: a strategy for targeting glutathione metabolism and enhancing ros-mediated therapy in triple-negative breast cancer treatment. *Small*. 2024;20(51):e2403861. doi:10.1002/smll.202403861
190. Wu L, Lin H, Cao X, et al. Bioorthogonal Cu single-atom nanozyme for synergistic nanocatalytic therapy, photothermal therapy, cuproptosis and immunotherapy. *Angew Chem Int Ed Engl*. 2024;63(27):e202405937. doi:10.1002/anie.202405937
191. HOU J, Bao H, Wang Y, et al. A hybrid alloying nanozyme-glutathione inhibitor co-delivery system initiates a dual-disruption on cancer redox homeostasis. *Small*. 2025;21(1):e2407555. doi:10.1002/smll.202407555
192. Shi Y, Bu W, Chu D, et al. Rescuing nucleus pulposus cells from ROS toxic microenvironment via mitochondria-targeted carbon dot-supported Prussian blue to alleviate intervertebral disc degeneration. *Adv Healthc Mater*. 2024;13(8):e2303206. doi:10.1002/adhm.202303206
193. Li Y, Liu J. Nanozyme's catching up: activity, specificity, reaction conditions and reaction types. *Mater Horiz*. 2021;8(2):336–350. doi:10.1039/D0MH01393E
194. Jiang Z, Li Y, Wei Z, et al. Pressure-induced amorphous zeolitic imidazole frameworks with reduced toxicity and increased tumor accumulation improves therapeutic efficacy In vivo. *Bioact Mater*. 2021;6(3):740–748. doi:10.1016/j.bioactmat.2020.08.036
195. Zhang D, Song J, Jing Z, et al. Stimulus responsive nanocarrier for enhanced antitumor responses against hepatocellular carcinoma. *Int J Nanomedicine*. 2024;19:13339–13355. doi:10.2147/IJN.S486465
196. Park JY, Lee HB, Son SE, et al. Determination of lysophosphatidylcholine using peroxidase-mimic PVP/PtRu nanozyme. *Anal Bioanal Chem*. 2023;415(10):1865–1876. doi:10.1007/s00216-023-04590-1
197. Park Y, Gupta PK, Tran VK, et al. PVP-stabilized PtRu nanozymes with peroxidase-like activity and its application for colorimetric and fluorometric glucose detection. *Colloids Surf B Biointerfaces*. 2021;204:111783. doi:10.1016/j.colsurfb.2021.111783
198. Liu Y, Ding L, Chen G, et al. A thermo-sensitive hydrogel with prominent hemostatic effect prevents tumor recurrence via anti-anoikis-resistance. *J Nanobiotechnology*. 2024;22(1):496. doi:10.1186/s12951-024-02739-3
199. Yang Y, Du J, Gan J, et al. Neutrophil-mediated nanozyme delivery system for acute kidney injury therapy. *Adv Healthc Mater*. 2024;13(26):e2401198. doi:10.1002/adhm.202401198
200. Xu J, Wu M, Yang J, et al. Multimodal smart systems reprogramme macrophages and remove urate to treat gouty arthritis. *Nat Nanotechnol*. 2024;19(10):1544–1557. doi:10.1038/s41565-024-01715-0
201. Wang Y, Xianyu Y. Nanobody and nanozyme-enabled immunoassays with enhanced specificity and sensitivity. *Small Methods*. 2022;6(4):e2101576. doi:10.1002/smtd.202101576
202. Jiang B, Fang L, Wu K, et al. Ferritins as natural and artificial nanozymes for theranostics. *Theranostics*. 2020;10(2):687–706. doi:10.7150/thno.39827
203. Huang R, Zhou X, Chen G, et al. Advances of functional nanomaterials for magnetic resonance imaging and biomedical engineering applications. *Wiley Interdiscip Rev Nanomed Nanobiotechnol*. 2022;14(4):e1800. doi:10.1002/wnan.1800
204. Białas K, Moschou D, Marken F, et al. Electrochemical sensors based on metal nanoparticles with biocatalytic activity. *Mikrochim Acta*. 2022;189(4):172. doi:10.1007/s00604-022-05252-2
205. Feng Y, Qin J, Zhou Y, et al. Spherical mesoporous Fe-N-C single-atom nanozyme for photothermal and catalytic synergistic antibacterial therapy. *J Colloid Interface Sci*. 2022;606(Pt 1):826–836. doi:10.1016/j.jcis.2021.08.054
206. Teplonogova MA, Volostnykh MV, Yapryntsev AD, et al. Switchable nanozyme activity of porphyrins intercalated in layered gadolinium hydroxide. *Int J mol Sci*. 2022;23(23):15373. doi:10.3390/ijms232315373
207. Han X, Li B, Wang W, et al. Cerium vanadate nanozyme with ph-dependent dual enzymatic activity for glioblastoma targeted therapy and postradiotherapy damage protection. *ACS Nano*. 2024;18(30):19836–19853. doi:10.1021/acsnano.4c06616

208. Hu J, Zheng Y, Yin C, et al. A novel and facile oxygen-activated time-temperature indicator with wide temperature monitoring range and good stability based on the laccase-like nanozyme. *Anal Chim Acta*. 2024;1330:343272. doi:10.1016/j.aca.2024.343272
209. Zhang M, Shao S, Yue H, et al. High stability Au NPs: from design to application in nanomedicine. *Int J Nanomedicine*. 2021;16:6067–6094. doi:10.2147/IJN.S322900
210. Zhang Y, Yu W, Zhang L, et al. Nanozyme-based visual diagnosis and therapeutics for myocardial infarction: the application and strategy. *J Adv Res*. 2024;2024:1.
211. Shi Y, Li H, Chu D, et al. Rescuing nucleus pulposus cells from senescence via dual-functional greigite nanozyme to alleviate intervertebral disc degeneration. *Adv Sci (Weinh)*. 2023;10(25):e2300988. doi:10.1002/advs.202300988
212. Ma X, Hao J, Wu J, et al. Prussian blue nanozyme as a pyroptosis inhibitor alleviates neurodegeneration. *Adv Mater*. 2022;34(15):e2106723. doi:10.1002/adma.202106723